MoDOT

Research, Development and Technology Division

RDT 99-001
Final Report

Temperature-Dependent Performance of Polymer Concrete Wearing Surface System on the Poplar Street Bridge

RI 90-16

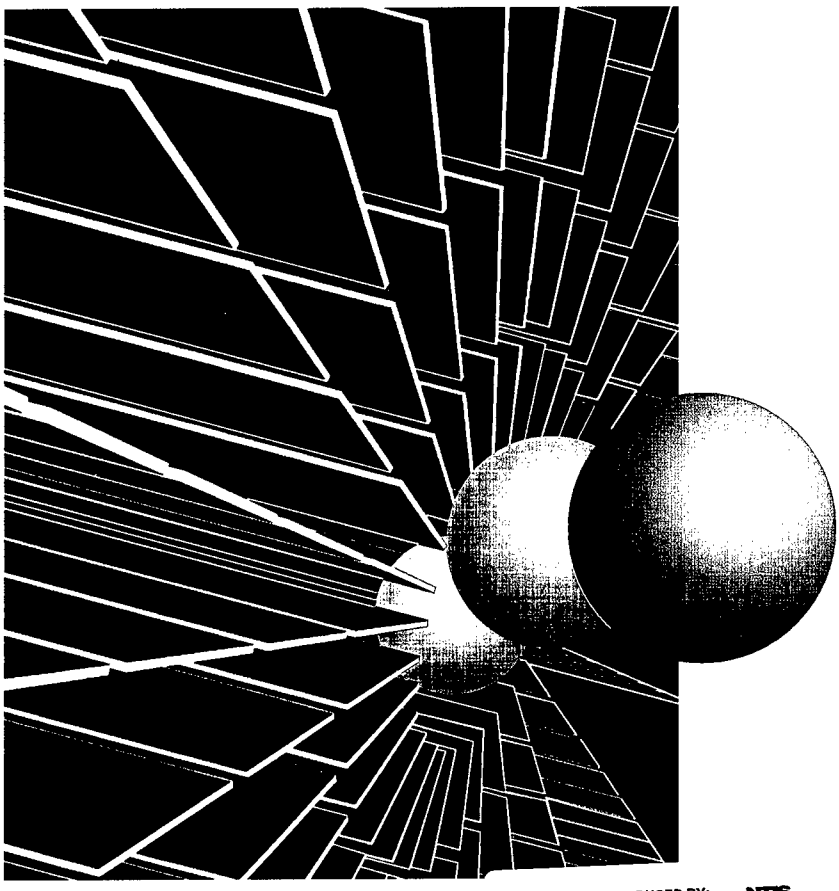

January, 1999

TEMPERATURE-DEPENDENT PERFORMANCE OF POLYMER CONCRETE WEARING SURFACE SYSTEM ON THE POPLAR STREET BRIDGE

Final Report
January 1999

Prepared for
Missouri Department of Transportation

by
Vellore S. Gopalaratnam
James W. Baldwin, Jr.
Wei-Min Cao

Department of Civil and Environmental Engineering
University of Missouri-Columbia

in cooperation with
Federal Highway Administration

TABLE OF CONTENTS

SUMMARY v

ACKNOWLEDGEMENTS vi

CHAPTER 1 – INTRODUCTION 1
1.1 Background information 1
1.2 Summary of previous related research conducted at MU 3
1.2.1 Field strain measurements 4
1.2.2 Flexural fatigue tests 4
1.3 Summary of inspections and field testing 6
1.3.1 Pull-out tests 7
1.3.2 Resistivity tests 7
1.3.3 Miscellaneous observations 9
1.4 Organization of the report 10

CHAPTER 2 –RESULTS FROM THE EXPERIMENTAL PROGRAM 15
2.1 Scope and motivations 15
2.2 General information 16
2.2.1 Materials 16
2.2.2 Polymer concrete specimen fabrication 16
2.2.3 Test procedure for static flexural and compression tests 17
2.2.4 Temperature control program 19
2.2.5 Data acquisition program 19
2.3 Compressive response of polymer concrete at different test temperatures 20
2.4 Flexural response of polymer concrete at different test temperatures 23
2.5 Flexural fatigue response of polymer concrete at different test temperatures 28
2.5.1 Stress level and range 28
2.5.2 Procedures for flexural fatigue tests 30
2.5.3 Data acquisition program 30
2.5.4 Flexural fatigue strength of PC and the influence of temperature 32
2.5.5 Progressive stiffness degradation of PC beams 36
2.5.6 Modes of failure at the different test temperatures 39
2.5.7 Effect of loading rate on the modulus of elasticity of PC 39
2.6 Potential crack repair procedures and their evaluation 40
2.6.1 Background information on the repair alternatives investigated 40
2.6.2 Details of the composite specimen for crack-repair tests 41
2.6.3 Specimen fabrication 43
2.6.4 Precracking and crack-repair procedures 43
2.6.5 Crack-repair tests 46
2.6.6 Temperature control program 47
2.6.7 Data acquisition program 47
2.6.8 Evaluation of the crack-repair procedures 49

CHAPTER 3 – WEARING SURFACE STRESS ANALYSIS 53
3.1 Scope and motivations 53
3.2 Possible reasons for transverse cracks in the wearing surface 53
3.3 Stresses in the PC wearing surface due to traffic loads 56
3.3.1 Wheel load and loaded area dimensions 56
3.3.2 The concept of influence line 56
3.3.3 Analysis of bending moment in the deck plate 57
3.3.4 Analysis of stresses in the wearing surface 60
3.4 Computation of thermally induced stresses in the PC wearing surface 61
3.4.1 Idealized structural model for thermal stress analysis 62
3.4.2 Analysis of stresses in the composite strip 64

CHAPTER 4 – CONCLUSIONS AND RECOMMENDATIONS 71
4.1 Conclusions 71
4.2 Recommendations 73

LIST OF REFERENCES 75

SUMMARY

The report details a five-year study of the performance of the epoxy (polymer) concrete wearing surface placed on the orthotropic steel-plate deck of the Poplar Street Bridge in St. Louis, Missouri. This study involved inspections, field testing and laboratory experiments and analyses. During the first few years, the focus was on the field study components. Later when some cracks were observed on the wearing surface, a detailed experimental and analytical investigation was incorporated to understand the cause of the cracks and study potential crack-repair procedures. Laboratory experiments were undertaken to study the temperature-dependent mechanical properties of the polymer concrete materials used on the bridge deck. Experiments included a series of static flexural tests, axial compression tests and flexural fatigue tests on the polymer concrete specimens under three different test temperatures. Temperature-dependent mechanical properties such as modulus of rupture, compressive strength, modulus of elasticity and fatigue strength were obtained from the tests. The analyses components focussed on the reasons for longitudinal fatigue cracking and transverse wearing surface cracking. It has been shown that a combination of traffic loads resulting in transverse bending of the deck plate and cold temperatures contribute to the longitudinal fatigue cracking observed on the deck. Transverse cracking of the wearing surface in the thickness transition zone of the eastbound lanes has been attributed to differential thermal expansion of the two webs of the south box girder coupled with thermal and elastic mismatch between the wearing surface and the steel deck plate. It has been concluded that temporary repair of wearing surface cracks using Pavon (asphalt-based product) or MMA sealant would minimize potential water infiltration onto the steel deck and extend the life of the wearing surface. An alternate repair approach where SIMCON (Slurry infiltrated steel fiber mat reinforced concrete) plates are bonded to the wearing surface holds promise as a long-term solution.

ACKNOWLEDGEMENTS

The Department of Civil Engineering, University of Missouri-Columbia (MU) conducted the work reported here. It was jointly sponsored by the Missouri Department of Transportation (MoDOT) and the Federal Highway Administration (FHA). Dr. Vellore S. Gopalaratnam and Dr. James W. Baldwin, Jr. were the Principal Investigators.

The authors would like to acknowledge the assistance provided over the years by Mr. Pat Martens and his maintenance crews (District 6 – MoDOT) in carrying out the inspections and field-testing. Thanks are also due to Mr. Al Laffoon, Mr. Shyam Gupta, Mr. Dan Salisbury and Mr. Paul Porter of the Bridge Division, MoDOT, who were responsible for our participation in the challenging and interesting five-year project.

Mr. Rich Brittin, Mr. Mike Stenko and Mr. Arthur Dinitz of Transpo Industries, Inc. provided useful discussions and contributed materials required for some of the experiments detailed in this report.

Last but not the least, the authors wish to acknowledge instrumentation support provided by Mr. Richard Oberto, MU College of Engineering and machining support provided by Mr. Rick Wells, MU Department of Civil Engineering. Students working on the project at various times include Mr. Robert Rigdon, Dr. Bryan Hartnagel, Mr. Wei-Min Cao, Dr. Zeyad El-Shakra, Mr. Ted Krull, Mr. Michael Holder, and Mr. Michael Rossi.

CHAPTER 1 – INTRODUCTION

1.1 Background information

The Poplar Street Bridge across the Mississippi River in St. Louis is an orthotropic steel-plate deck bridge, Fig. 1.1. The bridge carries three interstate highways, I-70, I-64, and I-55. It consists of two independent bridges supported on a set of common piers. One bridge carries four lanes of eastbound traffic; the other carries four westbound lanes. Each bridge is supported in the longitudinal direction by two box girders, which have web spacing of 5-ft. 5-in, and are spaced at 32-ft. 6-in. centers, Fig. 1.2. The box girder depth is 16-ft., except in the center span and over the two central piers, where they are 17-ft. and 25-ft, respectively. Cross-frames are used to distribute unsymmetrical loading to both girders and to enhance the torsional stiffness of the bridge. The steel deck plate thickness is typically 9/16- in. The plate is stiffened by a series of longitudinal stiffeners. These trapezoidal stiffeners are 11-in. deep and spaced at 26-in centers (stringer spacing on 13 in. centers). The transverse floor beams, spaced at 15-ft. centers, are also used to carry traffic loads transferred from the bridge deck. As the rigidities of the longitudinal stiffeners and transverse floor beams are not equal, the elastic properties in the two orthogonal directions are different. Consequently, the complete structural system is known as orthogonal-anisotropic, or, orthotropic bridge, [1].

The Poplar Street Bridge was constructed in 1967. The first wearing surface system consisted of two half-inch layers of epoxy and one one-and-half inch layer of rubberized asphalt concrete wearing surface. Stone chips were embedded in the second layer of epoxy as an anchor for the rubberized asphalt layer [2]. This wearing surface system was serviceable until 1983. It was then replaced by a new wearing surface that was designed to be identical to the original surface. The second wearing surface, however, lasted for only three years and was replaced by the third wearing surface in 1986. This time, a new proprietary system involving a fiberglass mat was added to the asphalt wearing surface layer. In early 90's, this third wearing surface system was also in need of replacement due to the unacceptable amount of rutting and shoving. Possible traffic-related reasons for the rapid deterioration of the second and third wearing surfaces cited [2] include (i) increased allowable tire pressures, (ii) larger allowable gross weights, (iii) increased traffic volume,

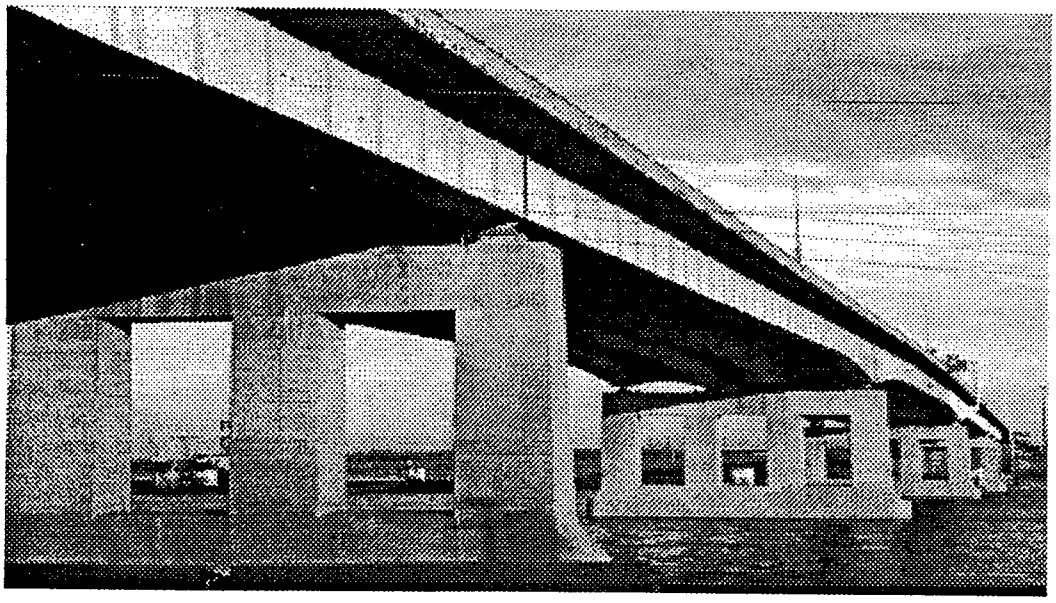

Fig. 1.1 The Poplar Street Bridge, St. Louis, Missouri

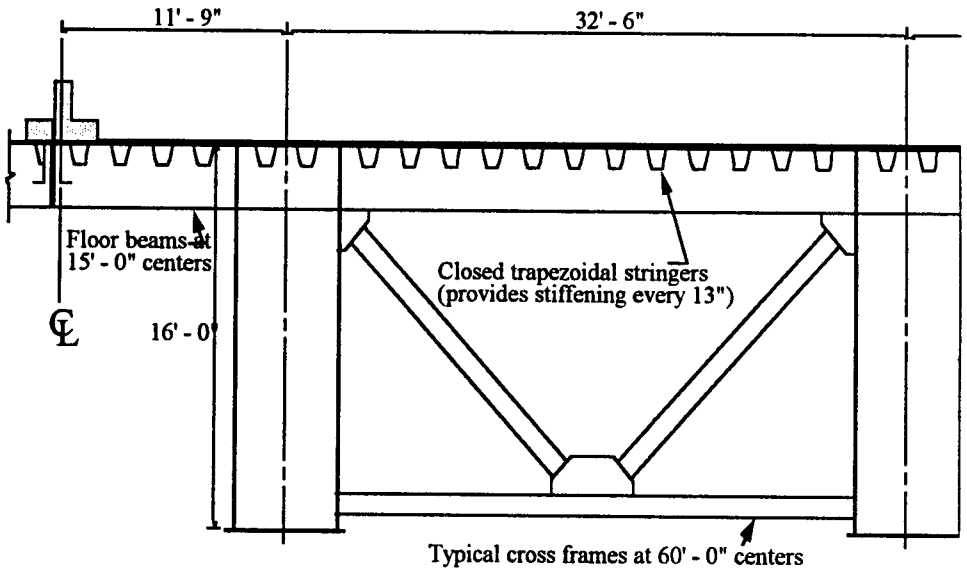

Fig. 1.2 Schematic structural details of the Poplar Street Bridge

and (iv) increased braking forces resulting from higher speed limits. Also contributing to the failure was the fact that the replacement wearing surfaces were placed while the bridge was open to traffic compared to original wearing surface which was placed on virgin metal deck under zero-traffic loads.

The Missouri Department of Transportation (MoDOT) awarded the Civil Engineering Department at the University of Missouri--Columbia (MU) a research contract to evaluate several asphalt and polymer concrete (PC) wearing surface systems that would satisfy the enhanced performance requirements. As a result of this study [2], T-48 Epoxy concrete supplied by Transpo Industries, Inc., New Rochelle, N.J., was selected for the wearing surface. This epoxy-based PC was placed on the bridge deck in August 1992. Since the margin of safety against potential cracking due to a combination of fatigue and thermal loads was less than desired, a program of inspection and field-testing was recommended [2].

This final report is based on results from the five-year follow-up study sponsored by MoDOT [3-8] including inspections, field-testing and a series of associated laboratory experiments and analyses to supplement observations from the field component of the study.

1.2 Summary of previous related research conducted at MU

The MU Department of Civil Engineering conducted an experimental study during 1989-92 to evaluate the performance of several alternate wearing surface materials [2, 9, 10]. The purpose of the study was to aid MoDOT in the selection of a new wearing surface for the Poplar Street Bridge in St. Louis, Missouri. Following this initial study, regular field inspections were conducted during 1992-97 after the construction of new PC wearing surface system (August 1992) to evaluate the in-service performance of the material. Results from the earlier studies are briefly summarized in the following subsections to provide the reader with a comprehensive overview of the Poplar Street Bridge research project. This includes laboratory studies, field strain measurements, wearing surface inspections on the bridge and field testing.

1.2.1 Field strain measurements

Field strain measurements were conducted to measure the in-service peak stresses experienced by the wearing surface. These stresses were used in the selection of suitable loading limits in the laboratory fatigue tests to simulate the in-service conditions. The strain data also provided information about the daily traffic patterns, and the number of times the absolute maximum strain event occurred on the bridge deck each day. Strain gages were fixed to the underside of the deck plate inside the south box girder of the eastbound bridge (Fig. 1.3). A personal computer-based data acquisition program was developed to collect the strain data over a period of six weeks. The measured peak strain experienced by the bridge deck was between 237 με and 250 με, and it was estimated that there were about 10 events each week of this range of magnitude of strain.

Using elastic analysis, a peak deck strain value of 250 με, the geometric data of the composite system, and the modular ratio between the PC wearing surface and steel deck, the maximum tensile stress in the wearing surface over the stiffener was calculated. This computation yielded the maximum wearing surface stress of 1,895 psi at cold temperature range (0°F - 35°F), and 995 psi under high temperature exposures (100°F - 165°F) [10].

1.2.2 Flexural fatigue tests

The laboratory flexural fatigue test formed the core part of the earlier investigation [2, 9]. Steel – PC composite beams simulating the actual steel deck-plate with the PC wearing surface were tested in flexural fatigue with simultaneous variation in the test temperature to simulate service conditions. The loading fixtures, instrumentation and specimens were all placed in a temperature-controlled chamber during fatigue testing. Up to four specimens were subjected simultaneously to thermal and flexural fatigue loading. Thermal loading simulated the daily and seasonal temperature changes experienced by the Poplar Street Bridge deck and varied sinusoidally between 160°F and 0°F. Six wearing surface materials were evaluated in the test program. These included two types of asphalt concrete and four types of PC. The 5-Hz laboratory fatigue tests were used to evaluate the susceptibility of the wearing surface materials to cracking or delamination types of failures.

The lower limit of the fatigue load was 150 lb. and the upper limit of the fatigue load was 1,150 lb. These loading levels simulated the maximum in-service stresses produced on

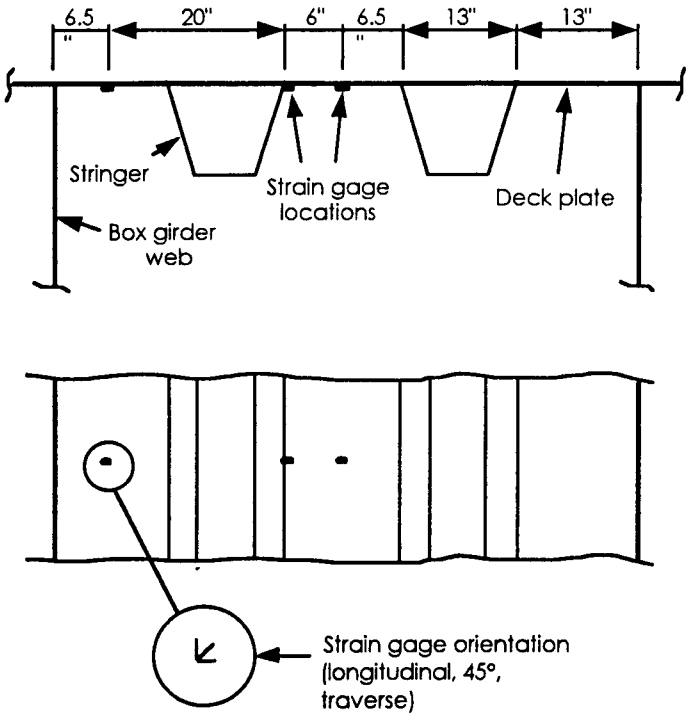

Fig. 1.3 Locations along one cross-section for strain measurements inside the south box girder

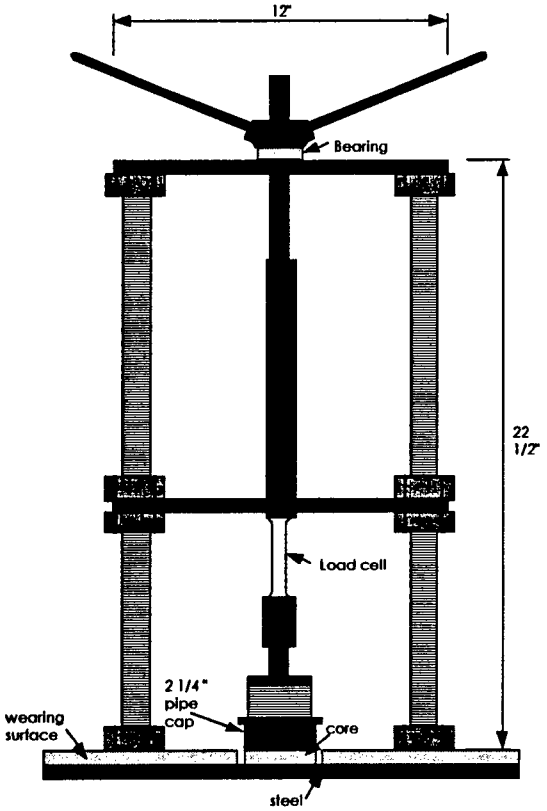

Fig. 1.4 Schematic of the pull-out loading and load-monitoring device

the wearing surface which were obtained from the field strain measurement component of the investigation [10]. It was observed that all the PC specimens exhibited cracking failures when the test temperature reached 0°F. Hence, in addition to the fatigue tests conducted with simultaneous sinusoidal variations in the test temperatures, flexural fatigue tests on the composite specimens were also conducted at a constant temperature of 0°F. The upper limit load was incremented by 150 lb. from 300 lb. after every 70,000 loading cycles until the specimen failed. It was observed that an upper limit load of 1,350 lb. caused specimen failure. The corresponding maximum tensile stress in the PC was computed as 1,375 psi for test temperatures between 100°F to 165°F, and 2,338 psi for test temperatures between 0°F to 35°F based on the variations in the elastic modulus of PC with test temperature.

Test sections of the various wearing surface materials studied were also placed on the bridge deck to evaluate the field performance of these materials. Among the six wearing surface materials tested, Transpo T- 48 epoxy-based polymer concrete performed the best in both components of the laboratory fatigue tests and field studies [2]. Transpo T- 48 PC was subsequently recommended for the new wearing surface system. Long-term inspection and monitoring of the wearing surface was also recommended since the margin of safety against cracking, particularly at cold temperatures, was small.

1.3 Summary of inspections and field testing

The MU Department of Civil Engineering also conducted field inspections on a yearly basis since the new PC wearing surface system was placed on the bridge deck in August 1992. Several additional unscheduled inspections, as needed, were also undertaken during the five-year period since. The purpose of this part of the investigation was to monitor the in-service performance of the new PC wearing surface. The inspection and field-testing were conducted on four 200-ft test sections, two on the east-bound and two on the west-bound lanes. The exact locations were identified in conjunction with MoDOT and are:

Test Section A	Right eastbound lane (Lane 4) from station 21+00 to 23+00
Test Section B	Right middle eastbound lane (Lane 3) from station 35+00 to 37+00
Test Section C	Left westbound lane (Lane 1) from station 37+00 to 35+00
Test Section D	Right middle westbound lane (Lane 3) from station 25+00 to 23+00

Inspections and field testing typically consisted of several components described in the following subsections.

1.3.1 Pull-out tests

Pull-out tests were performed in accordance with ACI 503R [11] to evaluate the tensile bond strength between the wearing surface and steel deck-plate (Fig. 1.4). Six pull-out tests were typically conducted at each test section during the yearly inspections [4-7]. Two-inch diameter cores were drilled on the wearing surface at predetermined locations. Steel pipe-caps were glued to the surface of the wearing surface. After adequate curing of the glue, pull-out load was applied to the wearing surface core using a loading frame equipped with a strain-gage based load cell. The load cell was connected to a strain gage conditioner to provide continuous readings of the applied load as well as the peak pull-out load.

The average value of the pull-out peak stresses recorded during the tests was about 500 psi. With very few exceptions, all the failures were at the glue-line between the pipe-cap and the wearing surface and not due to a failure of the wearing surface from the steel bridge deck plate. This indicated that the tensile bond strength between the steel deck and PC wearing surface was in excess of 500 psi. Another observation from the pull-out tests was that the pull-out loads were sensitive to test temperature. This was attributed to the temperature dependent properties of the epoxy glue used to bond the pipe-cap to the wearing surface. A lower test temperature typically resulted in a higher pull-out load [4-7].

1.3.2 Resistivity tests

Resistivity tests were conducted in accordance with ASTM D 3633-88 [12] at eighteen predetermined locations in each test section during the yearly inspections. Soap water saturated sponge was placed on top of the wearing surface at the desired location. A thin copper plate was placed on top of the sponge. Resistivity readings between the copper plate and the steel deck (through the wearing surface) were obtained using an ohm meter (Fig. 1.5). Low resistance values indicated the presence of cracks in the wearing surface at the test location. With the exception of those readings recorded directly over the visible cracks, all of the resistivity data obtained from the tests were significantly larger than 700,000 Ω, which represented acceptable performance of the PC membrane [4-7].

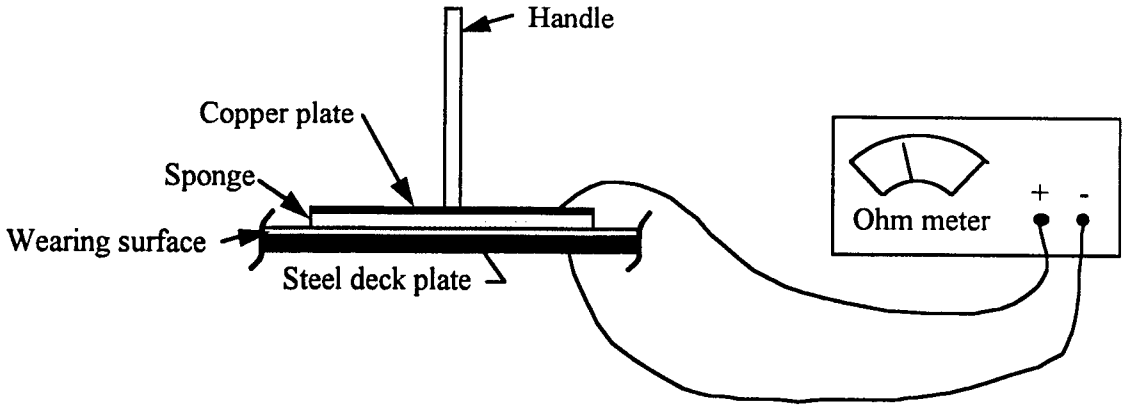

Fig. 1.5 Schematic of the resistivity test set-up

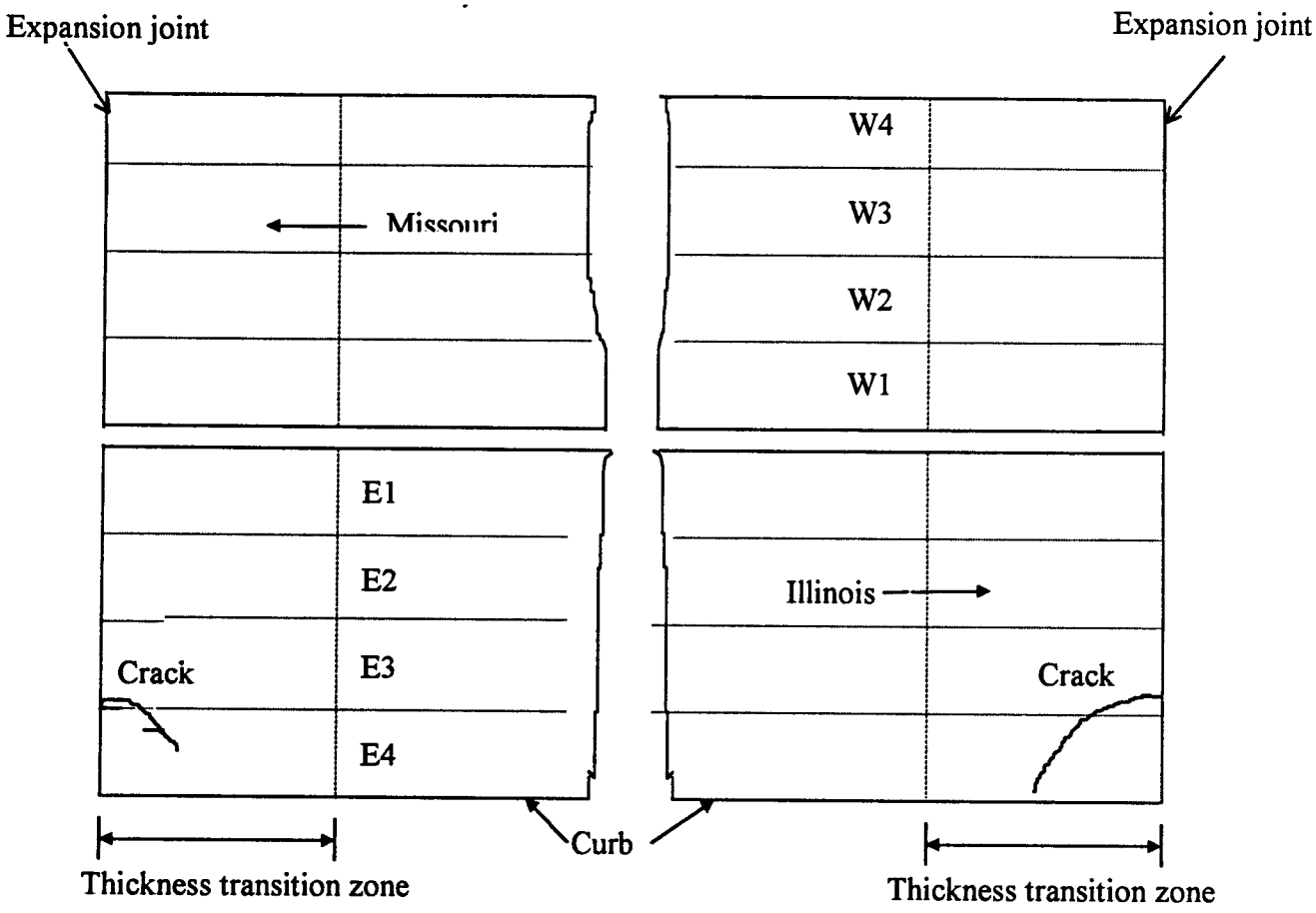

Fig. 1.6 Schematic of the transition-zone cracks in Lane 4 of the eastbound bridge first observed in June 93.

1.3.3 Miscellaneous observations

Chain-drag tests conducted in accordance with ASTM D 4580-86 [13] were used to identify potential areas of delamination between the wearing surface and the steel deck-plate. However after the first few inspections it became evident that this test was not very effective on the orthotropic steel deck bridge as the noise level on the deck from traffic was significant and masked small differences in acoustic signals from pockets of delamination.

Loss of top aggregates and visible damage to the wearing surface were also routinely monitored. The visual inspection included not just the four test sections, but the entire bridge deck.

Exhaustive inspections and field-testing were completed in September 92 [4], June 93 [5], September 94 [6], September 95 [7], September 96, May 97 and November 97. In addition, unscheduled visual inspections were also conducted in June 95 and May 96. The first inspection conducted in September 92 was completed approximately one month after the wearing surface was placed. No noticeable aggregate loss, cracking or other damage to the wearing surface was observed during this inspection. Two transverse wearing surface cracks one each at the two end regions (thickness transition zones where thickness of the wearing surface changes from 0.5 in. to 2.5 in. over a length of approximately 100 ft.) of eastbound Lane 4 were first observed during the inspection in June. 1993 (Lane E4, Fig. 1.6, [5]). These cracks were repaired in October 1993 using the Transpo T – 71 methyl methacrylate (MMA) crack sealant. In September 94, it was observed [6], that the crack repair procedures were only partially effective, in that while the repaired cracks had not grown in size (length and width), the reflected crack allowed water infiltration. Also during this inspection, a patch was observed 14 ft. east of Test Section C where the top layer of broadcast aggregates had debonded from the PC wearing surface. The problem was attributed to a local area of poor construction where the PC had already hardened prior to broadcasting of the layer of traction aggregates [6].

No significant further deterioration of the wearing surface was observed in the September 95 inspection. However, the Principal Investigators in consultation with bridge division MoDOT personnel decided to undertake [7] a laboratory study to investigate the cause of the transition zone cracks and potential ways to effectively repair cracks in the PC

wearing surface. This study related to the temperature-dependent mechanical performance of PC was considered even more relevant, given the increased number of cracks observed in the following three inspections [9]. During these inspections, a number of longitudinal fatigue cracks were observed in several lanes outside of the thickness transition zones. These cracks due to transverse bending were in the negative bending moment regions immediately above the longitudinal stiffeners and above the webs of the box girders. Additional transverse cracks were also spotted in the thickness transition zones at the west-end of the eastbound lanes. It was concluded that the transverse cracks were very likely the result of differential thermal expansion rather than due to fatigue loading from the traffic.

Chronological growth in the number and location of fatigue and transverse cracks are documented in Figs. 1.7-1.9. During the inspection in November 1997, the performance of three repaired patches (Fig. 1.9) were observed and judged to be in good condition. MoDOT maintenance crews had undertaken repair of these patches in September 1997 where the wearing surface had apparently lost the layer of top aggregates. The crew had removed the T-48 wearing surface over a rectangular saw-cut area, sand-blasted the deck and adjoining surfaces and placed a repair patch made using a comparable SIKA polymer product (commonly used in the repair of Portland cement concrete decks).

The additional laboratory investigation and cracking-related analysis presented in this report, not originally proposed, was viewed to be necessary and useful to understanding the causes of the different types of cracking observed during the inspections and also to study potential crack repair procedures. This final report focuses on these aspects of the project. Observations and recommendations are made on crack maintenance procedures wherever relevant.

1.4 Organization of this report

Experimental program conducted during this investigation and results from the tests are discussed in Chapter 2. Experiments include static compression and flexural tests on PC specimens at three different test temperatures, flexural fatigue tests on PC specimens at three different test temperatures, and flexural fatigue tests at the cold temperature on crack-repaired steel-PC composite specimens. Results from the analysis of the stresses in the wearing surface based on orthotropic deck theory due to traffic loads is reported in Chapter 3.

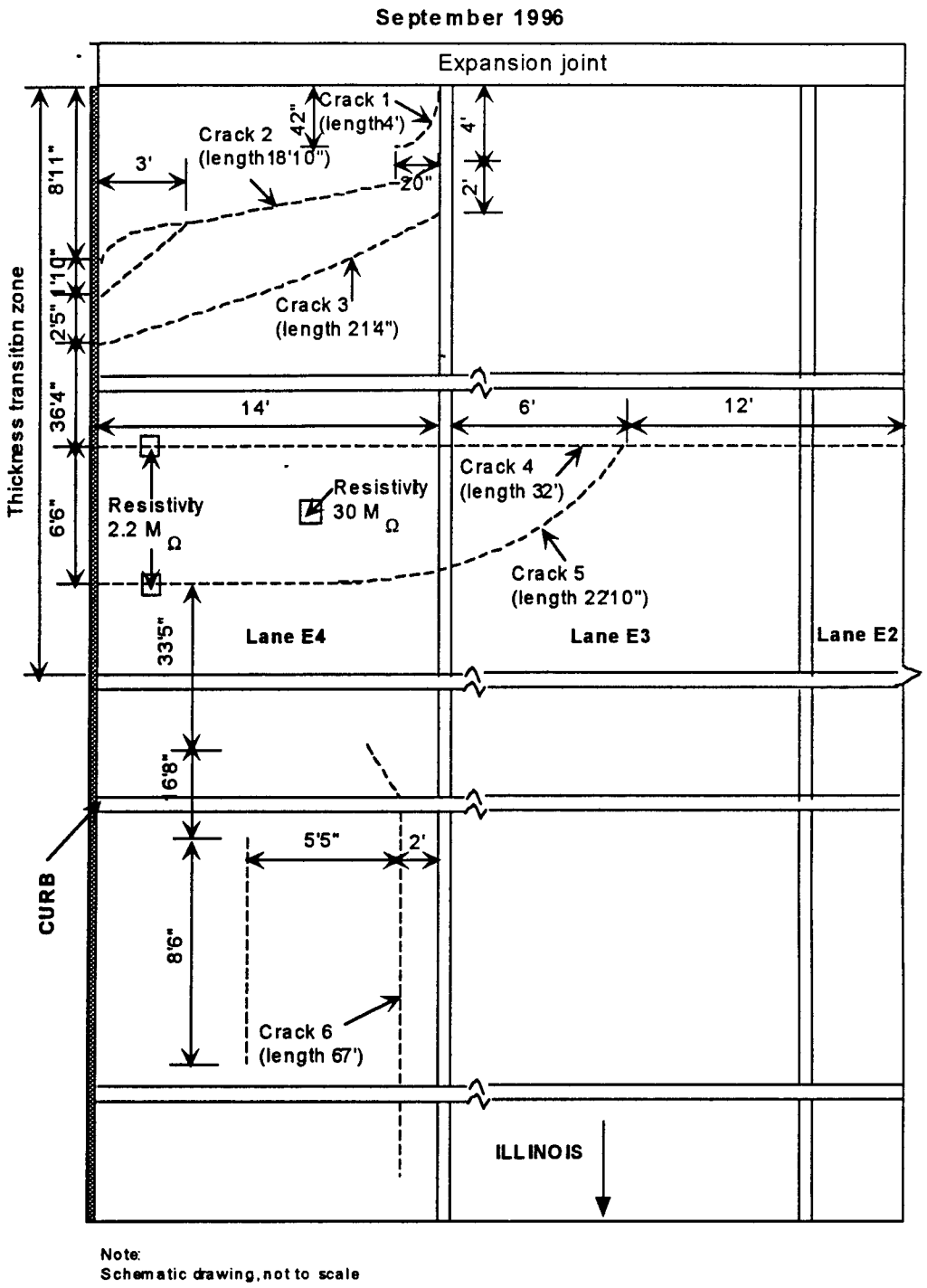

Fig. 1.7 Schematic drawing of the wearing surface cracks observed during the September 1996 inspection.

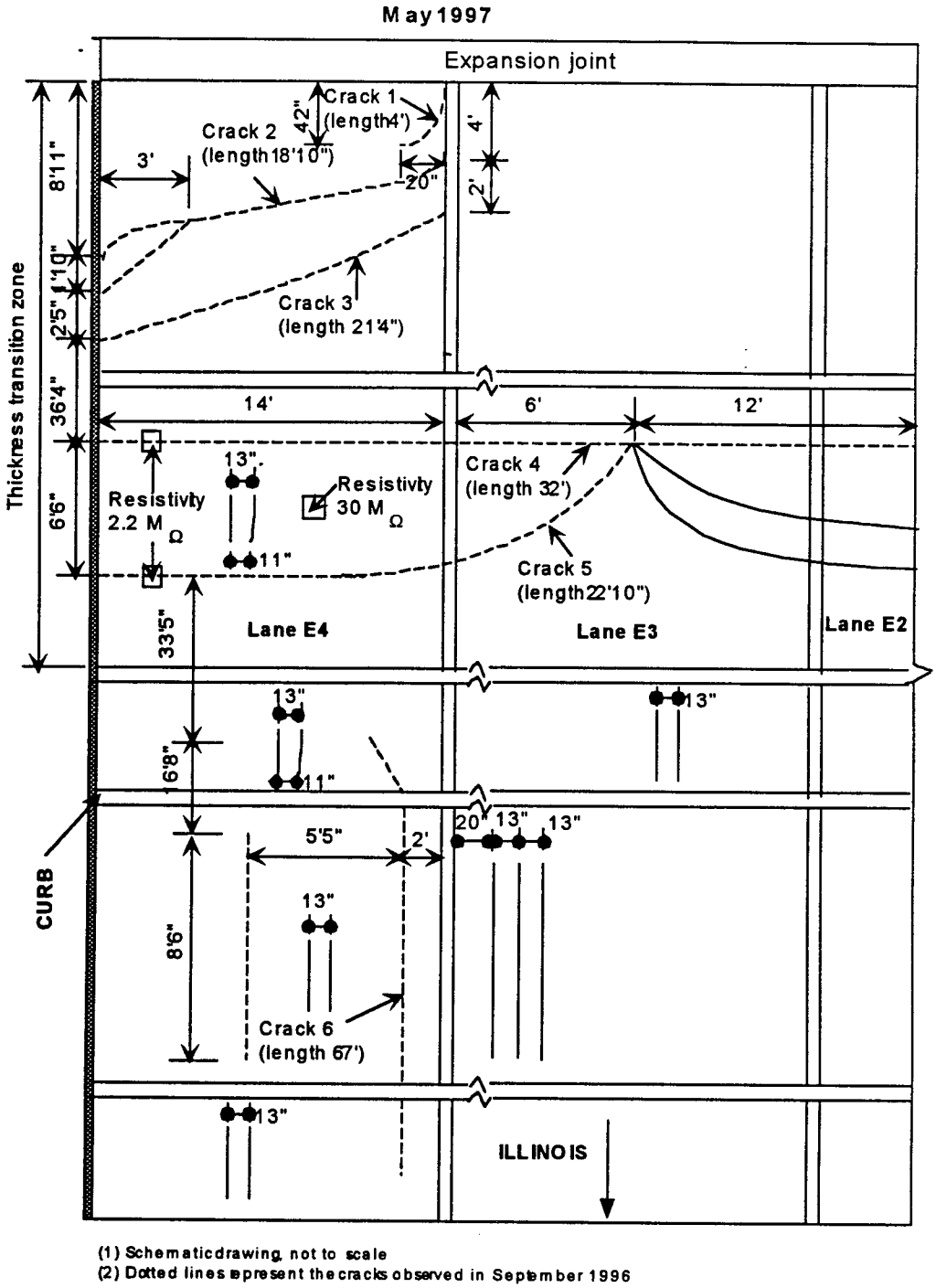

Fig. 1.8 Schematic drawing of the wearing surface cracks observed during the May 1997 inspection.

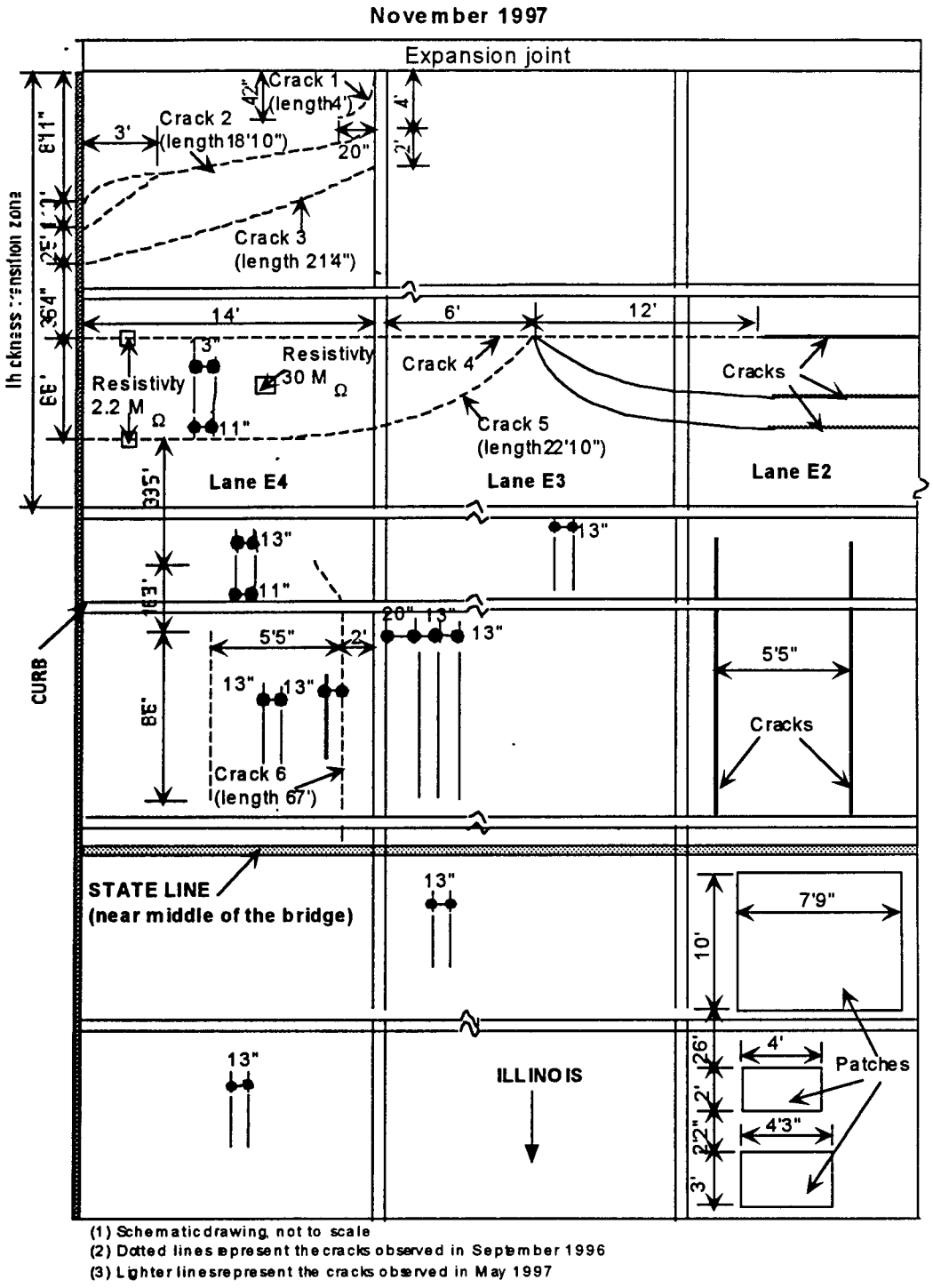

Fig. 1.9 Schematic drawing of the wearing surface cracks observed during the November 1997 inspection.

Chapter 3 also details stresses in the wearing surface due to thermal mismatch between the PC wearing surface and the steel deck and differential thermal expansion due to unequal expansion of the exterior and interior box girders. These stresses are reviewed in light of the results from the experimental program. Conclusions based on the experimental program and analysis are made in Chapter 4. The chapter also includes recommendations from this investigation.

CHAPTER 2 –RESULTS FROM THE EXPERIMENTAL PROGRAM

2.1 Scope and motivations

The experimental component of this study was motivated by the need to understand the causes for cracks in the wearing surface observed on the bridge during recent inspections. This component of the investigation focuses on the flexural performance of the PC specimens subjected to static and fatigue loading at different constant test temperatures. Additionally, the effectiveness of three potential crack repair approaches is also evaluated.

1. A number of static flexural and compression tests were conducted to evaluate the modulus of rupture, compressive strength, and modulus of elasticity of the PC material. Load-displacement relationships and differences in modes of failure were also studied in these tests. Static flexural and compressive tests were conducted at the following three steady-state test temperatures: 20°F (termed cold temperature), 73°F (termed room temperature), and 110°F (termed high temperature).
2. A series of flexural fatigue tests were conducted on PC beams at the same three test temperatures as the static flexural tests. Results from these tests were used to obtain the S-N relationship for the PC material at different constant temperatures. In addition, progressive stiffness degradation of the PC materials under flexural fatigue loading and flexural fatigue failure modes at different test temperatures were observed and analyzed. The fatigue characteristics of the PC material observed in this investigation is correlated with results from the previous studies [2, 9, 10] as well as with the cracking patterns observed in the field inspections [4-8].
3. There are no established procedures for repair of cracks in epoxy-concrete materials. This is mainly because once epoxy cures, it does not bond chemically with the subsequent layer of repair material. One has to rely on mechanical interlock to transfer loads from the newly placed material to the original cracked epoxy concrete wearing surface. This makes maintenance of a polymer (epoxy) concrete wearing surface difficult, particularly with regard to cracking. Three different crack repair approaches were studied as a part of this investigation. Statically precracked steel-PC composite specimens, simulating the cracked wearing surface system on the bridge, were repaired using a methyl-methacrylate, an asphalt-based material and a bonded fiber reinforced concrete plate. The

repaired specimens were subjected simultaneously to flexural fatigue loading and temperature variations to evaluate the service performance of these repair procedures.

2.2 General information

2.2.1 Materials

Transpo Industries, Inc., New Rochelle, New Jersey, supplied the T – 48 polymer concrete materials needed to fabricate the PC specimens used in this study. The PC material was similar to that used in the wearing surface for the Poplar Street Bridge. The Transpo T-48 polymeric binder consists of two parts of Part A, the epoxy resin, and one part of Part B, the hardener. Transpo T-48 epoxy resin is a viscous pale, yellow liquid with mild epoxy odor. It is a tough elastic resin and develops good bond with concrete, steel and aluminum deck surfaces. Aggregates broadcast on top of the PC provides for a non-skid-wearing surface. The hardener system is a pale, yellow liquid with amine odor. It is added to harden the epoxy resin base component. The filler is gray, odorless silica particles. Gradation of the aggregate used was identical to that used on the Poplar Street Bridge and was chosen to yield a minimum void volume that needs to be filled by the epoxy binder.

The following mix proportions prescribed by the manufacturer of the PC was used: Part A : Part B : Aggregates :: 19.6 lb. : 7.9 lb. : 120 lb. The content of each constituent, proportioned by weight, was 13.3 % epoxy resin, 5.4 % hardener, and 81.3 % aggregate.

2.2.2 Polymer concrete specimen fabrication

Steel molds of inside dimensions 2-in. x 2-in. x 10.25-in. were used to cast all the PC beams used in the flexural tests (static as well as fatigue specimens). All molds were wrapped with thin plastic sheet prior to casting to facilitate the demolding and clean-up process.

More than forty PC beams were fabricated in this study. The casting temperature was 73 ± 4°F (room temperature). The aggregate component was first weighed and placed in a stainless steel paddle-mixer. Sufficient amounts of epoxy resin and hardener were mixed together for approximately one minute. The neat PC mixture was then added to the aggregate, and mixed thoroughly for five minutes. The PC mixture was then placed into the steel molds in three layers. A vibrating table was used to compact the material during the casting process. After the placement of each layer, cutting and stabbing motion using wooden

stirrers removed air entrapped in the material. The top surface of the specimen was finished smoothly after the last layer of PC was placed. The entire fabrication process was completed within half-hour after initial mixing, and before the hardening of the material had commenced.

The PC beams were left in the mold for twenty-four hours to allow the material to set and cure. The molds were then disassembled to remove the specimens. All the beams were subsequently aged at the ambient temperature of 73 ± 4°F for more than six days before testing. This gave the PC material time to attain its prescribed physical properties.

The PC specimens used in the compression tests were cylinders of size 2-in. in diameter and 4-in. in length. Three specimens were cast in each batch. A thin film of silicone mold release was applied to lubricate the steel mold surfaces prior to casting. Material composition and casting procedures were the same as that used in fabricating the PC beams. To minimize potential eccentric loading, the ends of the PC cylinders were sanded flat and perpendicular to the cylinder axis before testing.

2.2.3 Test procedure for static flexural and compression tests

A 200-kip capacity MTS electro hydraulic, closed-loop servo-controlled testing system was used for the flexural and compression tests conducted in this study [8]. Four PC beams and three PC cylinders were tested at each of the three test temperatures in the static flexural and compression tests, respectively. The specimens were kept inside the testing chamber at the prescribed temperatures for four hours prior to testing so as to attain steady-state conditions.

All tests were performed inside a temperature controlled testing chamber. In order to evaluate the temperature effect on the mechanical properties of PC, all flexural and compression tests were conducted under the following three steady-state temperatures:

73 ± 2°F	Room Temperature
20 ± 2°F	Cold Temperature
110 ± 2°F	High Temperature

The temperature inside the testing chamber was controlled by using a refrigeration unit, a heater, blower fans and valves. Cold/hot damper valves were used to control the airflow in the heating and cooling circuits. Figure 2.1. shows a schematic of the test chamber

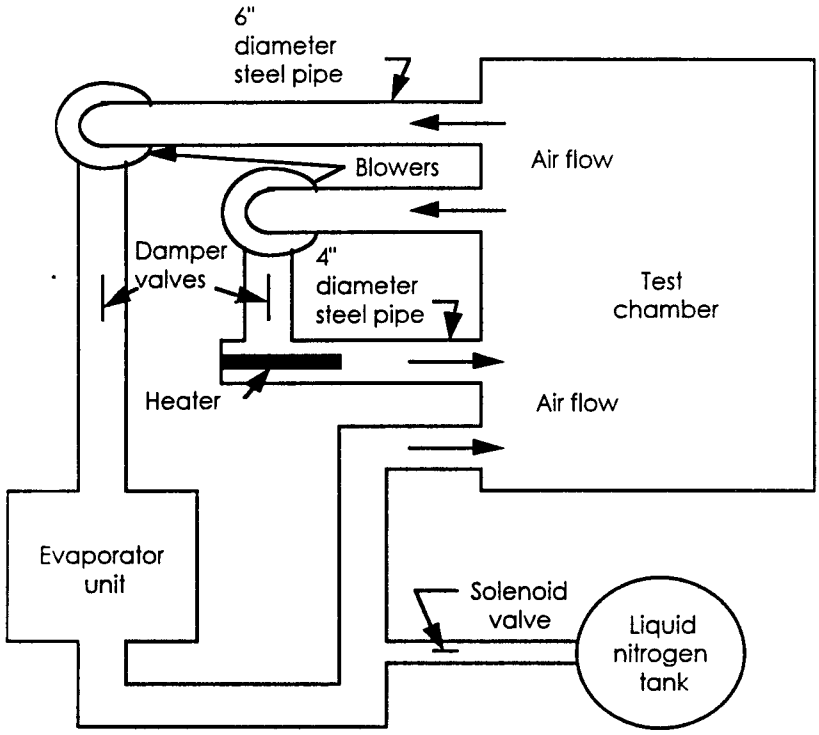

Fig. 2.1 Schematic of the temperature control chamber

and air flow paths. Additional details of the temperature chamber are described by Rigdon [9]. The liquid nitrogen tank and associated solenoid valve shown in Fig. 2.1 were not used in this investigation because the refrigeration (evaporation) unit provided all the cooling capacity required for the experiments described in this chapter.

2.2.4 Temperature control program

Temperature inside the testing chamber was controlled using a personal computer-based control system. Output signals from thermocouples placed at predesired locations inside the test chamber were input to the data acquisition system. The temperature command time histories were stored in a data file in a tabular format. After comparing the measured temperature with the prescribed temperature, the program sent control signals through the digital input/output lines to the appropriate device(s). This closed-loop arrangement facilitated simulating practical variations in test temperatures desired. In the present tests, the tabular values were all set at the desired constant value to produce cold temperature, room temperature or high temperature environment.

2.2.5 Data acquisition program

The test parameters including flexural load, compressive load, mid-span deflection (in flexural tests), and ram displacement (in compression tests) were recorded using the LabVIEW data acquisition software and an associated eight-channel data acquisition board. The input channels were scanned at a rate of one scan per second. The voltage signals acquired were converted to engineering units using appropriate calibration factors. The flexural load-mid-span deflection response (flexural tests), and compressive load–axial deformation response (compression tests) were plotted on the computer screen during the tests. The graphs were updated on-line after each scan. This facilitated monitoring of the mechanical response of the PC specimens even while they were enclosed in the temperature-controlled chamber during the tests.

2.3 Compressive response of polymer concrete at different test temperatures

Compression tests conformed to ASTM C 579 –93 procedures [14]. A 200-kip capacity load cell was used to measure the compressive load. The PC specimen was loaded between a fixed steel platen at the bottom and a swiveling steel platen on the top. The axial deformation of the specimen was recorded using an LVDT (linear variable displacement transducer) mounted on the hydraulic actuator.

The specimens were loaded at a constant deformation rate of 0.031 in./min. (room temperature tests), 0.015 in./min. (cold temperature tests) and 0.055 in./min. (high temperature tests) so as to provide approximately comparable "times to peak load". Tests were terminated when the specimen failed or when the compressive load dropped off to 75% of its peak value. Compressive strength and failure mode were recorded from the tests. Influence of test temperature on the compressive response of PC was studied. The results from the compression test on PC specimens are summarized in Table 2.1.

Figure 2.2 displays the comparison of compressive stress vs. ram displacement diagrams for specimens tested at three different temperatures. The variation of compressive strength with test temperature is shown in Fig. 2.3.

The compressive strength and compressive stress–strain (reflected from the ram displacement) response of the Transpo T-48 PC are greatly influenced by the test temperature (Fig. 2.2). The compressive strength and initial elastic modulus increases with a decrease in the test temperature. The average compressive strength for cylinders tested at 73°F was 4,760 psi. The ram displacement at peak compressive load increased with test temperature. The elastic modulus, E_c, for the PC cylinders obtained from the slope of the initial portion of the compressive response at room temperature was 3.22×10^5 psi which was only 6.4% smaller than the elastic modulus of PC obtained from the static flexural tests at the same temperature. The elastic modulus of PC at 110°F was significantly smaller at 20,666 psi. The average maximum compressive load sustained by the specimens tested at 20°F was 3.30×10^4 lb. Due to the significant deformations of the loading train at such loading levels, accurate modulus of elasticity could not be computed (at 20°F) from the ram displacement values recorded.

The compressive stress–ram displacement relationship of PC tested at room temperature was linear till the stress was approximately 50% of the strength. A transition to

Table 2.1 Results from static compression tests on polymer concrete cylinders[1]

Test temperature, T, (°F)	Compressive strength, σ_c, (psi) [2]	Relative compressive strength [3] σ_{Rc}	Initial elastic modulus, E_c, (psi) [2]	Failure mode
20	10,775 10,116 10,590	2.21	-- [5] -- [5] -- [5]	Large inclined cracks
	10,494 [4]			
73	4,795 4,847 4,637	1.00	3.50×10^5 2.46×10^5 3.70×10^5	Multiple fine inclined cracks
	4,760 [4]		3.22×10^5 [4]	
110	1,172 1,203 1,340	0.26	18,440 20,068 23,489	Large inclined cracks
	1,238 [4]		20,666 [4]	

1. Cylinder size (2" diameter, 4" length).
2. 1 MPa = 145 psi, 1 mm = 0.03937 in.
3. Ratio between the average compressive strength at prescribed temperature and that at reference temperature (73 °F).
4. Average values from tests on three specimens.
5. Values are inaccurate because of large deformations of steel bearing plates placed at the ends of the specimens.

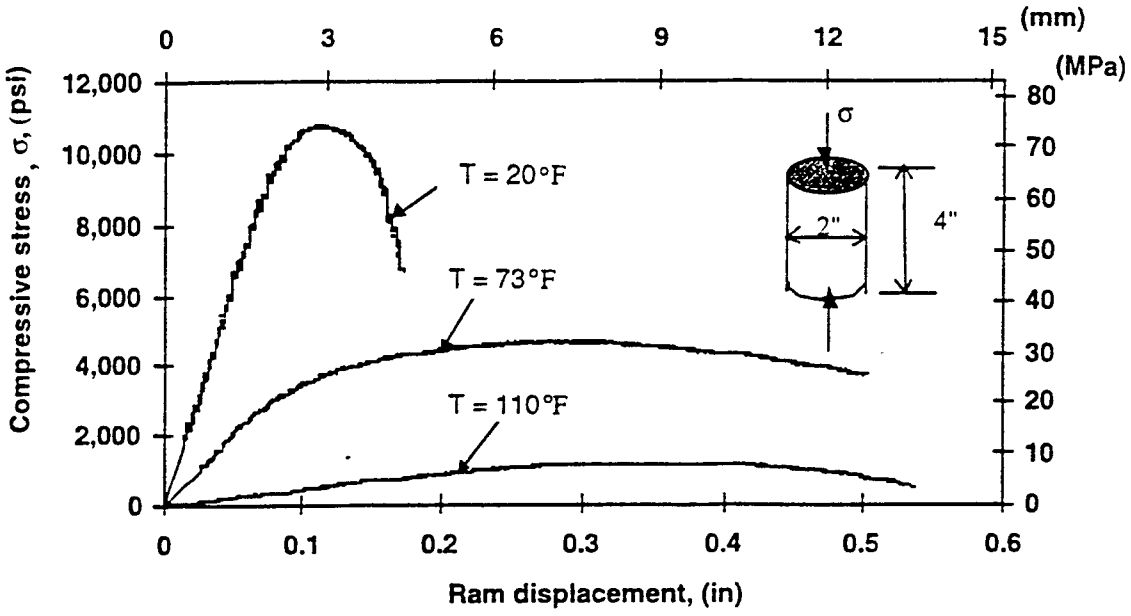

Fig. 2.2 Influence of temperature on typical compressive stress-ram displacement response of polymer concrete cylinder

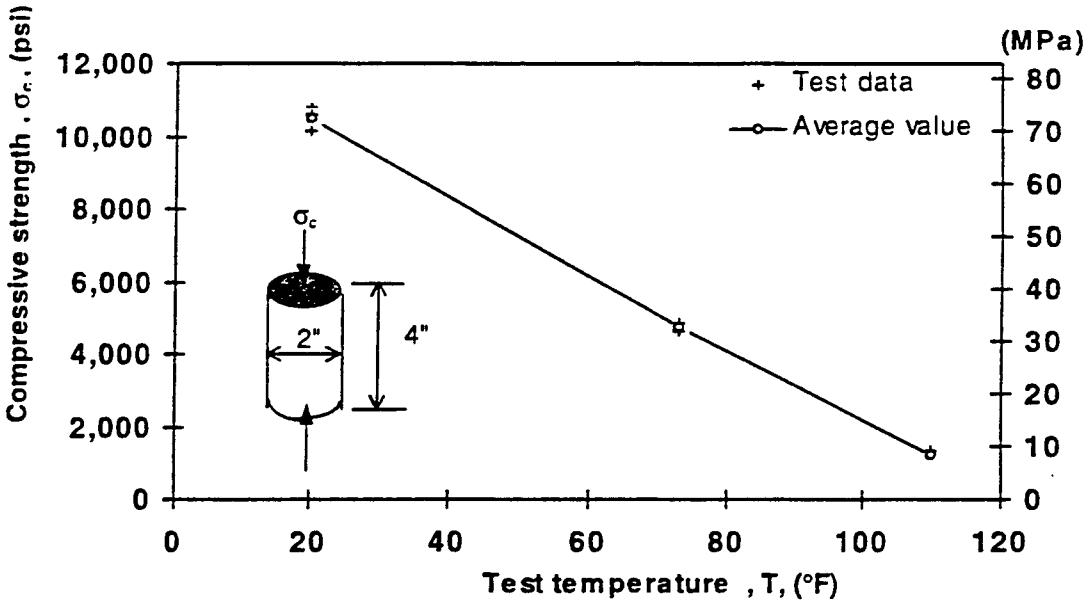

Fig. 2.3 Ultimate compressive strength as a function of test temperature

nonlinear response was then observed. The specimen experienced significant deformation in the nonlinear stage before failure. The PC cylinder at room temperature failed due to a system of multiple fine cracks inclined at 45° to the vertical axis. These cracks became visible immediately following the peak load (in the descending region). The deformation of the specimen continued after cracking but the test was stopped when the compressive stress dropped off to about 75% of its peak value. The compressive stress–ram displacement relationship for PC cylinder tested at 20°F exhibited a linear response almost up to the peak load. One of the three specimens broke in an abrupt, brittle mode after reaching its maximum stress. The other two also underwent a rapid loss of load carrying capacity after reaching the peak load, but did not fail catastrophically.

It is of interest to note that the specimens tested at 20°F and 110°F failed due to a limited number of large cracks along planes inclined at approximately 45° to the loading axis. The reason for the difference in the crack patterns among cylinders tested at three temperatures (large major cracks and multiple fine cracks) is not clear and requires further detailed study on the temperature-dependent microstructure of PC material. However, the observations from compression tests clearly indicated that failure in PC specimens tested at all three temperatures was due primarily to local shear failure on planes inclined at 45 ° to the axis of the cylinders.

2.4 Flexural response of polymer concrete at different test temperatures

Static flexural tests on PC beams were conducted in accordance with procedures specified by ASTM standard methods C 580 - 93: "Test Method for Flexural Strength and Modulus of Elasticity of Chemical - Resistant Mortars, Grouts, Monolithic Surfacings, and Polymer Concretes." [15]. The specimens were tested in simple bending with a 9 in. span. Flexural loads were applied to the beams at mid-span through aluminum load cells. The hydraulic ram was controlled to move upward at a rate of 0.024 in./min. (room temperature), 0.012 in./min. (cold temperature) and 0.030 in./min. (high temperature). Since the failure strain of PC increases as the temperature increases, the displacement rates chosen resulted in comparable "time to peak load" for the specimens tested at three different temperatures. The applied flexural load, mid-span deflection and ram displacement values were recorded in a spreadsheet data file at a rate of one scan per second. Flexural test was stopped when the

beam broke or the load dropped off to 75% of its peak value. The structural characteristics of the PC such as flexural strength, σ_f, initial elastic modulus, E_f, and the mid-span deflection at peak load, δ_f, were obtained from the test at each of the test temperatures. The influences of temperature on these properties were analyzed. The modulus of rupture values computed also served as the basis for selecting appropriate maximum stress levels to be used in the subsequent flexural fatigue tests on PC beams at the same temperature. Fig. 2.4 shows a schematic of the flexural test set-up.

The load cell consisted of an aluminum plate supported on a pair of rollers, a steel block glued to the mid-span of the plate, and a loading stub threaded into the steel block. A circular recess was machined at the mid-span of the deflection bar to accommodate the tip of the loading stub, thus preventing eccentric loading, Fig. 2.4.

Two strain gage-based deflection devices were held in place against the head plate on both sides of the beam. The readings of the two devices were averaged to give the mid-span deflection of the specimen during the flexural tests, Fig. 2.4.

Results from static are presented in Table 2.2. The modulus of rupture of PC beam was calculated assuming elastic behavior. The initial elastic modulus of PC, E_f, was also obtained from the initial linear portion of the load-mid-span deflection response. A typical flexural load vs. mid-span deflection response for a PC beam tested at room temperature is shown in Fig. 2.5. The load-deflection diagram was linear till the flexural load reached approximately 30% of its peak value corresponding to a deflection of about 0.02 in. The material exhibits a gradual transition to nonlinear response. It undergoes significantly large nonlinear deformations prior to failure.

PC specimens tested at room temperature failed as a result of a single vertical crack near mid-span. The cracks initiated from the top tension surface of the beam, and extended in the vertical direction toward the compression face. The specimens fractured in a brittle mode. The average static flexural strength at room temperature for Transpo T-48 PC, σ_f, was 3,198 psi and the average initial modulus of elasticity, E_f, was 3.44×10^5 psi. Figure 2.6 indicates that increase in test temperature causes a significant decrease in the static flexural strength of the PC material. Table 2.2. shows a 84% gain in the modulus of rupture of PC when the test temperature was reduced from 73°F to 20°F, and a 81% loss in strength when the temperature was increased from 73°F to 110°F. This variation of flexural strength of the

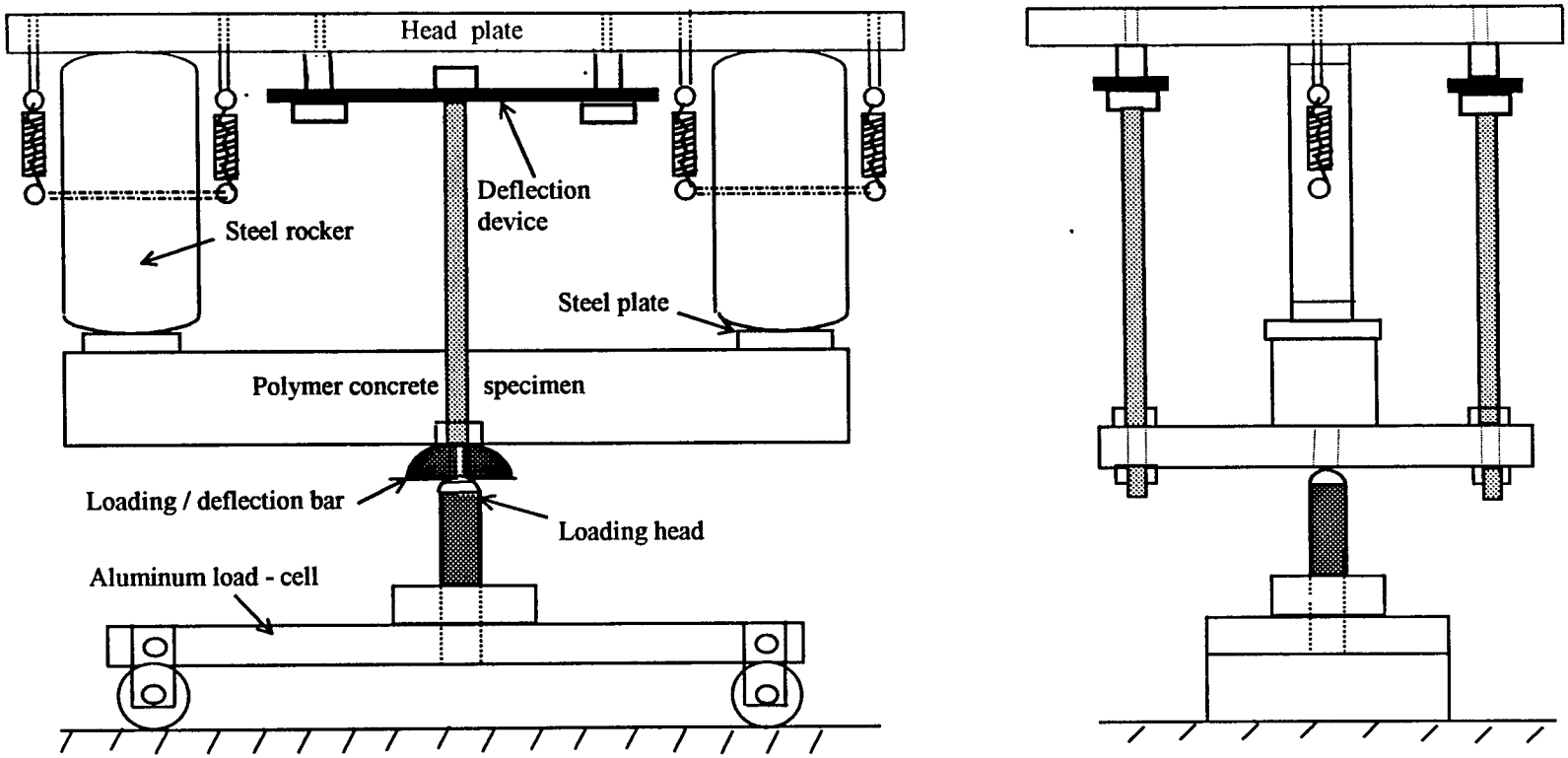

Fig. 2.4. Testing configuration for flexural tests on polymer concrete beams

Table 2.2 Results from static flexural tests on polymer concrete beams[1]

Test temperature, T, (°F)	Flexural strength σ_f, (psi) [2]	Relative flexural strength [3], σ_{Rf}	Initial elastic modulus E_f, (psi) [2]	Deflection at peak load, δ_f, (in) [2]	Failure mode
20	5969	1.84	9.40×10^5	0.048	Brittle failure
	5881		11.38×10^5	0.043	
	5946		10.05×10^5	0.045	
	5714		8.58×10^5	0.048	
	5878 [4]		9.85×10^5 [4]		
73	3256	1.00	3.37×10^5	0.171	Brittle failure
	3209		3.01×10^5	0.183	
	3111		3.37×10^5	0.168	
	3215		4.01×10^5	0.164	
	3198 [4]		3.44×10^5 [4]		
110	614	0.19	-- [5]	0.380	Softening failure
	602		-- [5]	0.355	
	613		-- [5]	0.393	
	591		-- [5]	0.348	
	605 [4]				

1. Beam size (2" x 2" cross-section, 10.25" length, tested over a 9" span, mid-point loaded).
2. 1 MPa = 145 psi, 1 mm = 0.03937 in.
3. Ratio between the average flexural strength at specified temperature and that at reference temperature (73°F).
4. Average values from tests on four specimens.
5. Values are inaccurate because of large deformation of the specimens at loading point and supports.

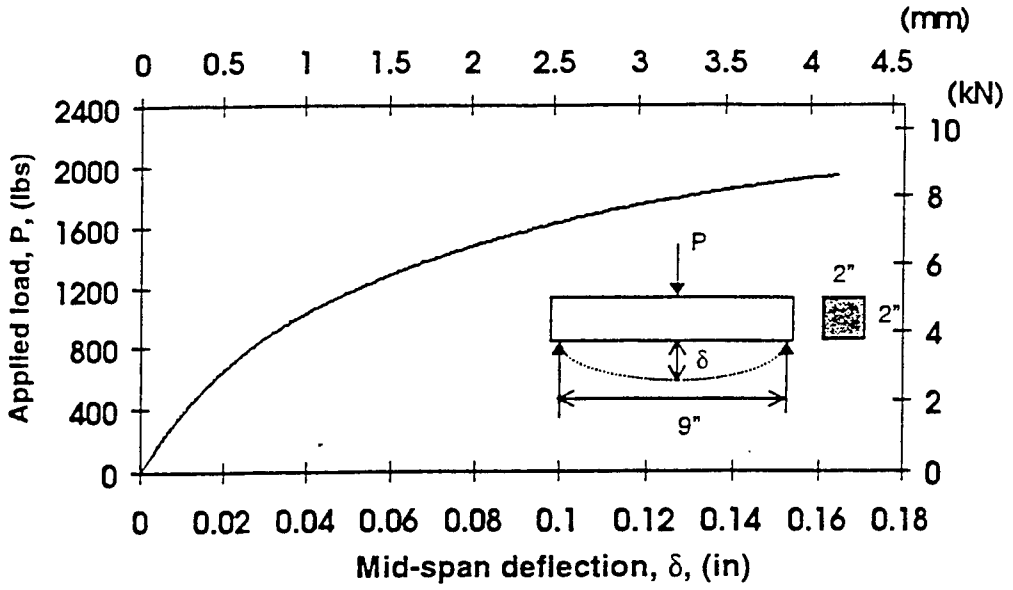

Fig. 2.5 Typical load-mid-span deflection response for beam tested at 73°F.

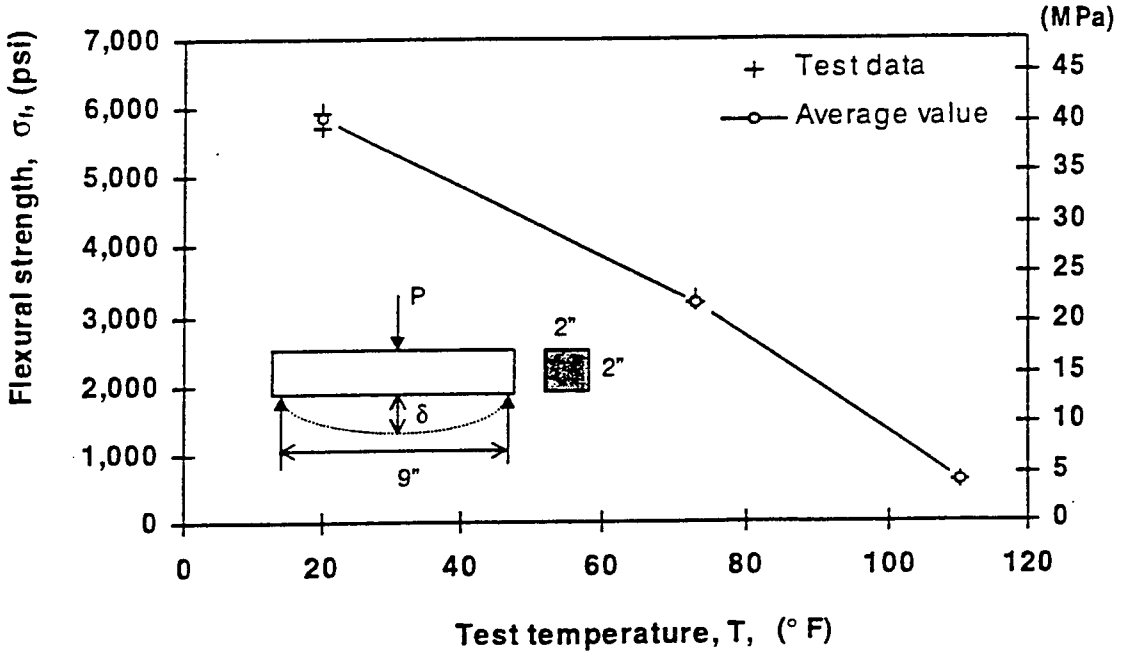

Fig. 2.6 Ultimate flexural strength as a function of test temperature.

Transpo T-48 PC with test temperature is representative of the thermally-sensitive nature of mechanical properties in such materials. The material loses most of its flexural strength at a temperature of 110°F.

As observed from Fig. 2.6 and Table 2.2, the scatter in the static flexural strength data at each of the three test temperatures is small. As the maximum stress levels used in the fatigue test were selected based on the average static flexural strength at the same temperature, the small scatter allows some measure of confidence in the fatigue stress range. The flexural load -- mid-span deflection responses for PC specimens tested at three different temperatures are plotted in Fig. 2.7. It indicates that in addition to flexural strength, the test temperature also has significant influences on the modulus of elasticity and load-deflection response of the PC. PC beams tested at 20°F exhibited a linear load-deflection relationship nearly up to the ultimate flexural load. Failure was sudden and due to a single vertical crack close to the midspan. The mid-span deflection of the specimen corresponding to peak flexural load was much less than that of the beam tested at 73°F, indicating brittle behavior of PC at cold temperatures. The average initial elastic modulus of PC at 20°F was 9.85 x 10^5 psi, an almost two-fold increase compared to its value at room temperature

Transpo T- 48 PC exhibited a softening behavior at 110 °F. The load–deflection response was nonlinear soon after flexural load was applied. PC beams tested at this temperature underwent significant amount of deformation before failure occurred. Since the specimens also experienced large local deformations at loading point and end supports, modulus of elasticity of PC at high temperature could not be computed accurately, and thus is not reported in Table 2.2. The mid-span deflection corresponding to ultimate flexural load was almost twice as much as that of PC at room temperature. The cracks for all beams tested at high temperature initiated at the tension face of the specimens, and propagated in a stable manner towards the compression face. At 110°F all PC beams failed in a softening mode.

2.5 Flexural fatigue response of polymer concrete at different test temperatures

2.5.1 Stress level and range

Ram displacement control was used to apply a 5 Hz sinusoidal flexural fatigue loading to the PC beam. For each of the three test temperatures, the maximum stress ratio, S_{max}, was selected as a fraction of the static flexural strength of PC, σ_f, at the same

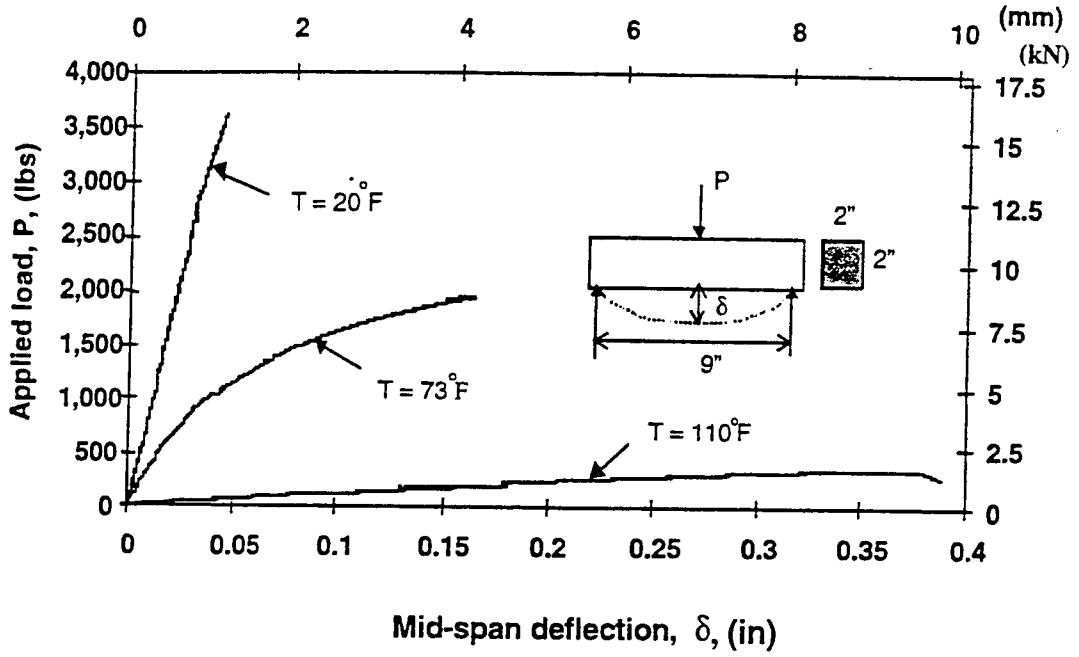

Fig. 2.7 Influence of temperature on typical load-deflection response of polymer concrete beams.

temperature. The values of S_{max} were 0.73, 0.63, 0.53 and 0.43 for the room temperature (73°F) and high temperature (110°F) tests. Preliminary tests showed that the fatigue life of PC at cold temperature (20°F) was considerably higher than its fatigue life at the other two temperatures. Therefore, the maximum stress ratios for cold temperature fatigue tests were selected as 0.77, 0.69, 0.61 and 0.53. This allowed the fatigue-testing program to be completed in a timely manner. Stress range, R, is defined as the ratio of S_{min}/S_{max}. A stress range of approximately 0.20-0.25 was used for all flexural fatigue tests. However, since the ram displacement range was adjusted manually to simulate prescribed load levels, the actual loading range varied somewhat from this value. The actually applied stress range for each specimen is included in Table 2.3. It should also be noted that the PC beam deformed considerably while being tested at a temperature of 110°F. Consequently, the applied loading range was continuously decreasing during the duration of the test. As a result, the mean value of the actually applied loading ranges is reported.

2.5.2 Test procedures for flexural fatigue

Cyclic loading was conducted at a constant frequency of five cycles per second (5 Hz) until failure of the specimen occurred. The ram (actuator) displacement was used as the feedback parameter. A haversine signal of 5 Hz frequency was sent from the function generator as the command signal. The set point of the hydraulic ram was manually adjusted to maintain the prescribed loading level and range during the test. The PC beams were loaded until they reached the fatigue limit, indicated by a rapid loss of load carrying capacity. The number of loading cycles to failure, N_f, and the mid-span deformation development of the beam were monitored for each test. The maximum stress ratio versus number of loading cycles to failure diagram, S_{max}-N_f diagram was obtained for all the test temperatures. Stiffness of the PC beam was monitored by determining the ratio between the amplitude of the cyclic load and the amplitude of the mid-span deflection. This ratio was also used to compute the initial elastic modulus of PC, E_f.

2.5.3 Data acquisition program

Flexural load, mid-span deflection and ram displacement were monitored using a National Instruments data acquisition board. A typical data acquisition cycle was initiated

Table 2.3 Results from flexural fatigue tests on polymer concrete beams

Test temp., T (°F)	Maximum stress ratio, S_{max} [1]	Relative stress ratio, S_{Rmax} [2]	Stress range, R [3]	Number of cycles to failure, N_f	Initial elastic modulus, E_f (psi) [4]	Deformation at failure (in) [4]	Failure Mode
	0.774	1.452	0.273	3,600	1,277,546	0.0258	Brittle
	0.689	1.293	0.198	7,925	1,283,126	0.0168	Brittle
20	0.697	1.307	0.201	8,600	1,246,702	0.0172	Brittle
	0.614	1.152	0.302	32,465	1,341,532	0.0208	Brittle
	0.625	1.173	0.216	24,660	1,273,109	0.0247	Brittle
	0.532	0.998	0.198	63,740	1,268,876	0.0338	Brittle
					1,281,815 [5]		
	0.737	0.737	0.213	3,828	886,100	0.182	Brittle
	0.754	0.754	0.213	3,795	752,801	0.390	Brittle
	0.630	0.630	0.203	5,055	715,784	0.336	Softening
73	0.630	0.630	0.209	5,225	748,784	0.327	Softening
	0.534	0.534	0.191	6,600	671,087	0.270	Softening
	0.533	0.533	0.193	9,870	700,629	0.205	Softening
	0.425	0.425	0.227	36,650	660,462	0.525	Softening
	0.413	0.413	0.213	25,595	701,071	0.258	Softening
					729,590 [5]		
	0.745	0.1409	0.249	4,835	53,840	0.318	Softening
	0.640	0.1211	0.250	6,950	53,559	0.362	Softening
110	0.650	0.1230	0.300	9,225	59,643	0.294	Softening
	0.561	0.1061	0.278	12,345	56,996	0.294	Softening
	0.568	0.1075	0.243	11,380	47,691	0.338	Softening
	0.460	0.0870	0.246	62,595	54,204	0.541	Softening
					54,322 [5]		

1. Maximum stress ratio values with respect to static flexural strength at the same test temperature.
2. Relative stress ratio computed as the ratio of maximum stress level at prescribed test temperature to the static flexural strength at reference temperature (73°F).
3. Stress range represents the ratio of S_{min} / S_{max}, where both S_{min} and S_{max} are at the prescribed temperature.
4. 1 MPa = 145 psi, 1 mm = 0.03937 in.
5. Average values from tests on specimens at the same prescribed temperature.

every five seconds. During each sampling cycle, fifty data points were acquired from each input channel using an acquisition rate of 250 scans per second (total acquisition time of 0.2 sec.). These data points constituted one full cycle of the sine wave representing a 5 Hz fatigue load or deflection signal. A subroutine of the data acquisition program was then used to fit a sine wave to this set of fifty data points through a least square curve fitting algorithm. The amplitude and phase shift of the signal were the output from this subroutine. Graphs on the computer screen were continuously updated to show the load and deflection signals as they were acquired. In addition, the stiffness of the beam and the maximum applied fatigue load were also displayed. This information allowed monitoring the progress of the test and control of the loading level and range.

2.5.4 Flexural fatigue strength of PC and the influence of temperature

Results from the flexural fatigue tests on PC beams are summarized in Table 2.3. Fig. 2.8 shows the S_{max} vs. N_f relationship for a PC beam tested at 73°F. The trend of the test data clearly shows that the number of loading cycles to failure decreases as the maximum stress level increases. Power equation of the form shown in Eq. 2.1, typically used for fatigue response, was used to obtain fits for the experimental data from this study. Such equations would be useful for later analytical investigations on fatigue cracking of the PC wearing surface.

$$\text{Log } N_f = A\,(S_{max})^B \tag{2.1}$$

Table 2.4 includes results obtained for the power-law fits at the various test temperatures. Results from the Wohler fatigue model calibrations were also attempted and are reported in [8]. The comparison of S_{max} vs. N_f response for specimens tested at three different test temperatures is presented in Fig. 2.9. These curves, from left to right, are for T = 73°F, T = 110°F, and T = 20°F. PC beams tested at cold temperature showed the highest fatigue life, and those tested at room temperature had the lowest fatigue life.

It should be noted that this comparison is based on maximum stress ratio. The maximum stress levels applied to the specimens at one of the three test temperatures were selected as a fraction of the modulus of rupture of PC at the same temperature. Figure 2.10 shows the comparison of the S_{max} vs. N_f relationships for beams tested at three temperatures

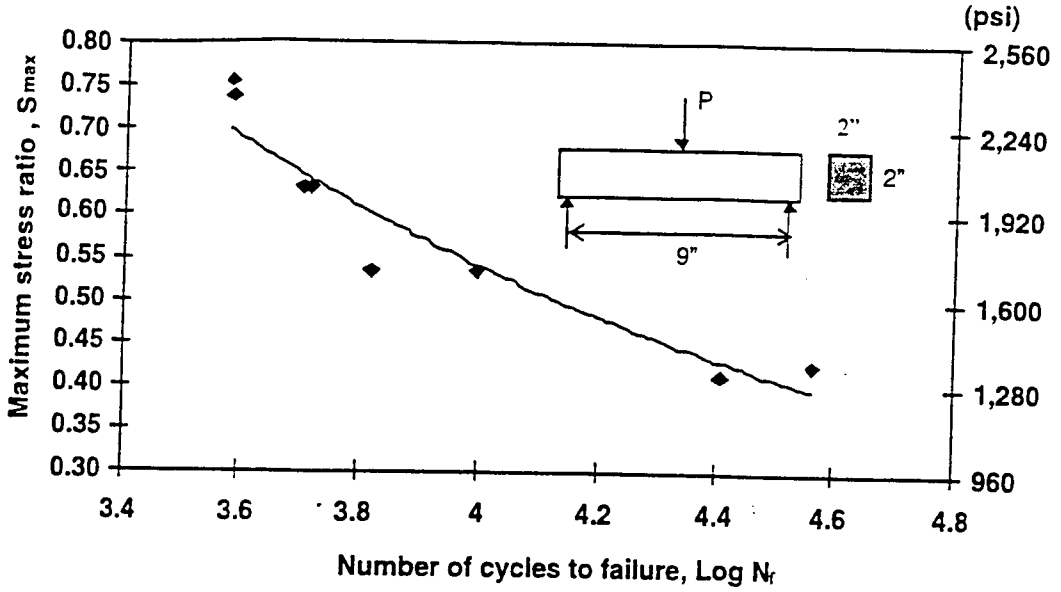

Fig. 2.8 $S_{max} - N_f$ relations for polymer concrete beam tested at 73°F.

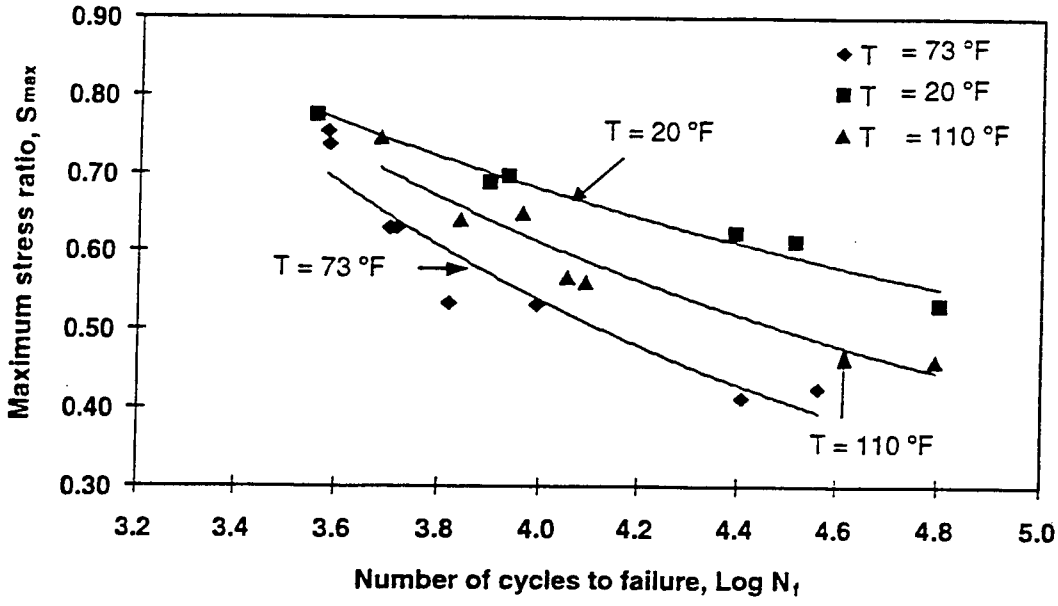

Fig. 2.9 Influence of temperature on the $S_{max} - N_f$ relations for polymer concrete beams.

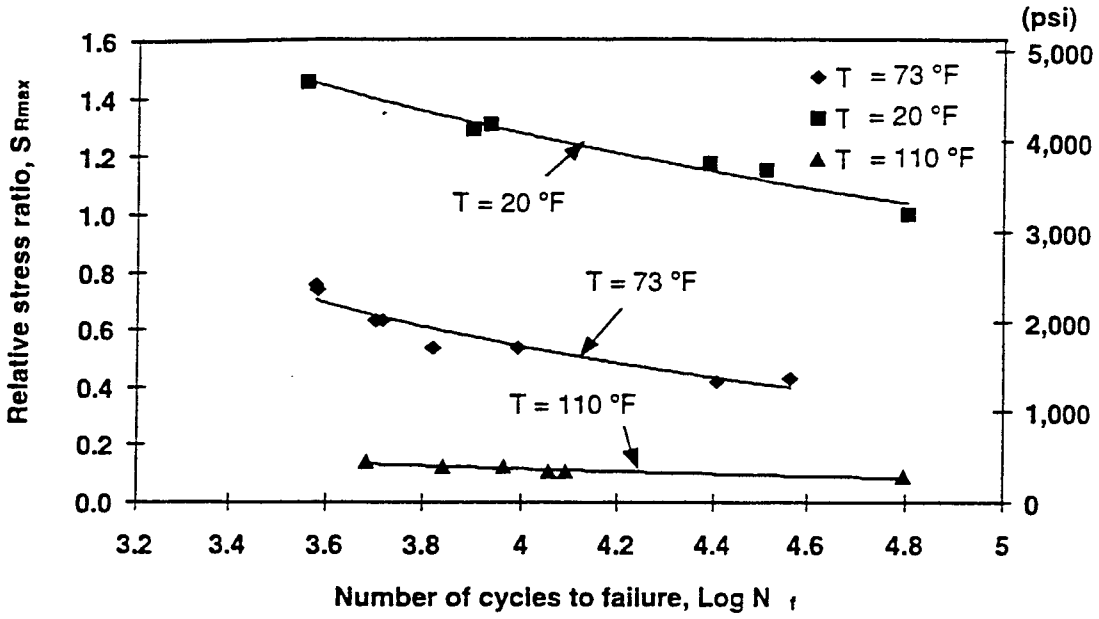

Fig. 2.10 Influence of temperature on the $S_{Rmax} - N_f$ relations for polymer concrete beams.

Table 2.4 Results for the power equation fits for fatigue test data

Test temperature T, (°F)	A[1]	B[1]	R^2 of the fit[1]
20	2.8950	-0.8444	0.9598
73	3.1355	-0.3910	0.9171
110	3.1355	-0.5261	0.9168

1. $\text{Log } N_f = A\ (S_{max})^B$

Table 2.5 Effect of loading rate on the modulus of elasticity of polymer concrete

Test temperature, T, (°F)	Initial elastic modulus from static test, E_f, (psi)	Initial elastic modulus from fatigue test, E_f, (psi)	Percentage increase of E_f (%)
20	985,000 [1]	1,281,815 [1]	30
73	344,000 [1]	729,590 [1]	112
110	20,666 [2]	54,322 [1]	163

1. Average value from flexural tests on a number of polymer concrete beams.
2. Average value from static compression tests on three polymer concrete cylinders.

using relative stress ratio. The relative stress ratio is defined as the ratio between the maximum stress level applied in fatigue test at the prescribed temperature divided by the average modulus of rupture of PC at a reference temperature of 73°F. PC beams tested at 73°F showed higher load carrying capacity than those at 110°F, even though the ratio of the load capacity in fatigue is less at 73°F.

2.5.5 Progressive stiffness degradation of PC beams

Figure 2.11 shows the mid-span deformation development diagram of a PC beam tested at 73°F. The maximum stress level applied to the beam was 63% of its static flexural strength. The mid-span deformation reflects the stiffness decrease of the specimen with respect to the fatigue loading cycles. The curve can be divided into three phases: Phase I shows an initial rapid increase of mid-span deformation due to crack initiation. The deformation of the PC beam approaches approximately 25% of its deformation at failure, with only approximately 10% of its fatigue life expended. The specimen then experiences a stable development of deformation due to steady-state crack growth in Phase II. The deformation of the beam increases linearly with respect to the fatigue loading cycles to approximately 90% of its fatigue life. Phase III showed rapid increase in deformation of the beam and unstable crack growth as it approaches its fatigue limit.

Figure 2.12 presents a comparison of the mid-span deformation development curves for the specimens subjected to three different maximum stress ratios (0.53, 0.63 and 0.75). All three beams were tested at room temperature. The deformation development diagrams for these beams show three stages similar to that observed in Fig. 2.11. The beam tested at higher stress level undergoes more rapid degradation in stiffness. Similar observations were valid for specimens tested at 110°F and 20°F. The influence of stress level on the final mid-span deformation at failure at a given temperature was not found to be significant,Table 2.3.

Figure 2.13 shows the comparison of the mid-span deformation diagrams for beams tested at three different test temperatures. The applied maximum stress ratio, S_{max} , was comparable (approximately 0.63) for all three beams. All specimens showed a large initial rate of deformation, a stable intermediate rate followed by a rapid rate at incipient failure. The final deformation at failure for specimens tested at 73 °F and 110°F appeared to be

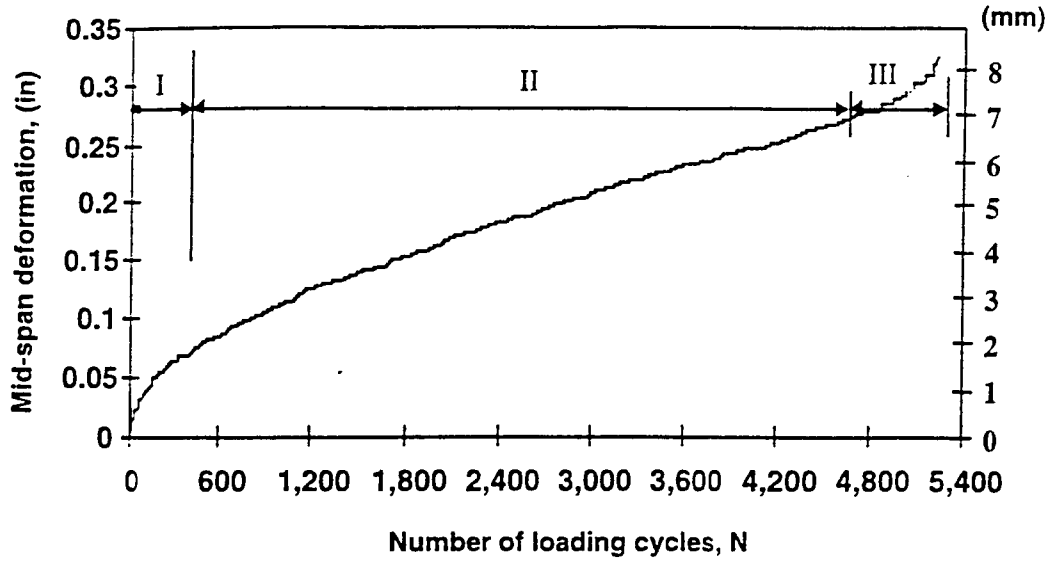

Fig. 2.11 Typical mid-span deformation development curve for a polymer concrete beam tested at 73°F (S_{max} = 0.63).

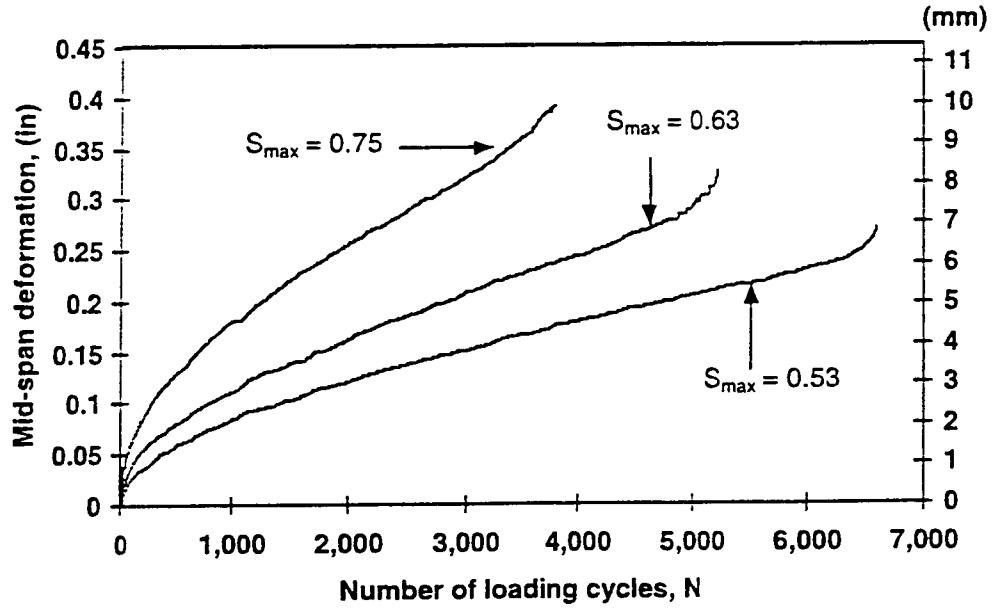

Fig. 2.12 Influence of stress level on the mis-span deformation development for polymer concrete beams tested at 73°F.

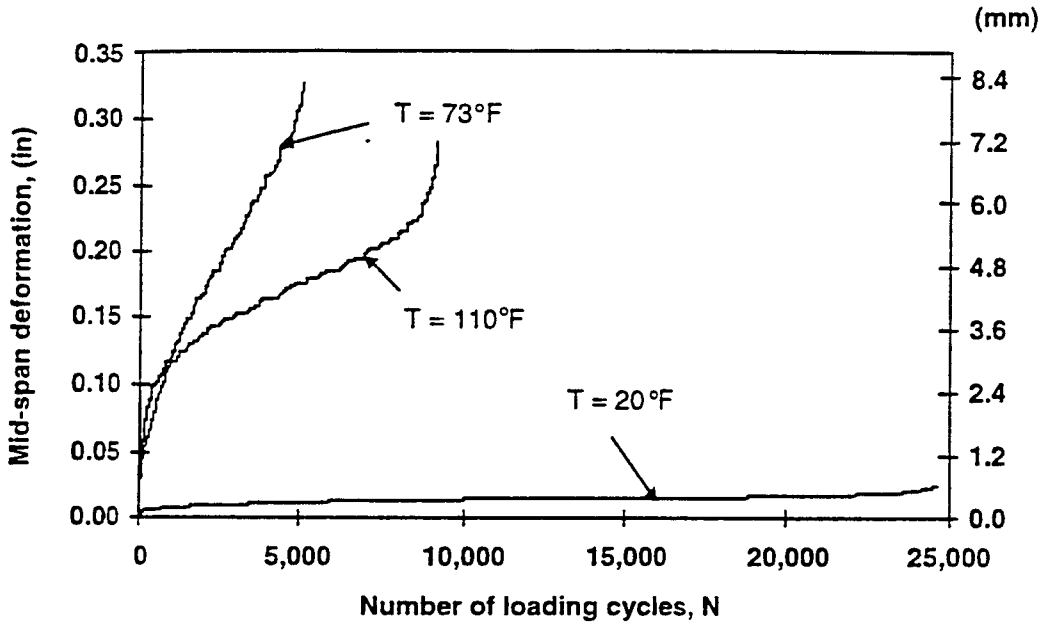

Fig. 2.13 Comparison of mid-span deformation development for polymer concrete beams tested at 20°F, 73°F, and 110°F (S_{max} = 0.63).

comparable. However, the deformation at failure for the PC beam tested at 20°F was about 0.03 in., almost an order of magnitude smaller deformation at failure compared to beams tested at the other two temperatures.

2.5.6 Modes of failure at the different test temperatures

All PC beams tested at cold temperature experienced a sudden, brittle flexural failure. These beams failed due to a single vertical crack occurring near midspan. All PC beams tested at 110°F had a gradual failure due to softening. The crack always initiated at the top tension face of the beam near the mid-span, and propagated vertically toward the compression face. PC beams tested at all temperatures exhibited a rapid increase in mid-span deformation as the specimens reached incipient failure.

Six of the eight specimens tested at room temperature underwent a softening type of failure. The other two beams, which were subjected to higher stress levels, experienced brittle failure. Since all PC beams in the static tests at room temperature exhibited brittle failure, it is probable that the change in failure mode from brittle (in static tests) to softening (in fatigue tests) for the six beams is due to an increase in internal temperature of the specimen during the fatigue tests. The cyclic loading at a frequency of 5 Hz generates heat energy in the PC beam. The flexural strength of PC decreases as the specimen temperature increases. Since the stress levels applied in fatigue tests were selected based on the flexural strength of PC obtained from the static tests at the same temperature, an overestimate of the flexural strength could result in measured fatigue life that is lower than the actual fatigue life of PC. This phenomenon was more obvious when the specimens were tested at lower stress levels. Longer fatigue life at the lower stress levels allowed accumulation of more internal heating due to fatigue cycling. The increase in specimen internal temperature due to fatigue cycling showed less notable effect on the specimens tested at 110°F, since this increase in internal heat was insignificant compared with the test temperature.

2.5.7 Effect of loading rate on the modulus of elasticity of PC

The initial modulus of elasticity of PC, E_f, was also computed from results obtained in the fatigue tests. It should be noted that the elastic modulus of PC computed from fatigue

loading data was based on load and deflection readings acquired from the initial few loading cycles (prior to any noticeable stiffness degradation).

One measure of the effect of the strain rate on the elastic modulus of PC is obtained by comparing the E_f obtained from the fatigue tests with that obtained from the static tests at the same test temperature (Table 2.5). The test results show that at all three temperatures, increasing loading rate results in an increase in the stiffness of the material. The average percentage gain for the E_f was 30% for the beams tested at 20°F, 112% for those tested at 73°F, and 163% for those tested at 110°F. The effect of loading rate on the elastic modulus of PC was more significant at higher test temperature. The change of stress level in fatigue tests at the same temperature was not found to cause noticeable variation in the elastic modulus of PC, since the resulting change in loading rate was comparatively small.

2.6 Potential crack repair procedures and their evaluation

2.6.1 Background information on the repair alternatives investigated

After exhaustive literature search for materials and procedures for repairing cracks in polymer concrete wearing surfaces, the research team narrowed down the potential alternatives to be investigated in the laboratory study to three. Two of them are essentially crack repair/sealing materials (Transpo T- 71 Methyl Methacrylate –MMA, and Pavon) while the third essentially uses a bonded overlay (Slurry Infiltrated Fiber Mat Concrete – SIMCON) type approach to rehabilitate the wearing surface. The crack-sealing approaches offer only a short-term solution that minimizes water and chloride infiltration on to the steel bridge deck. Cracks are typically reflected on the repaired surface after only a few hundred fatigue cycles. The bonded-overlay using SIMCON precast or cast-in-place plates offer a long-term solution and have to be applied on the entire deck. This alternative involves significantly more initial cost and effort. Several other issues need to be studied with this wearing surface repair option as discussed later in this section (greater stiffness, larger self-weight etc.).

Since epoxy does not chemically bond to any material once it is cured, one has to rely on mechanical bond to repair/seal cracks in these wearing surface materials. Mechanical bond can be achieved through aggregate interlock and friction. Alternately, any material that

has expansive characteristics during curing (instead of one that exhibits shrinkage) would be ideal for sealing cracks in epoxy as one could introduce moderate amounts of prestressing force across the crack to seal it effectively. A repair material that has a low viscosity would be able to better penetrate fine fatigue cracks observed in the PC wearing surface. Also since the orthotropic deck is very flexible, a low-modulus material (modulus lower than that of the wearing surface preferred) would be ideal for crack repair in the wearing surface. The Transpo T-71 (a MMA material) and Pavon (a bituminous material) materials possessed many of the characteristics desired in a crack repair material. The Transpo T-71 MMA, like the T-48 PC wearing surface is a polymeric material, and hence has characteristics compatible with the wearing surface (similar modulus material with thermal characteristics and strain-rate sensitive mechanical response). The Pavon material is a low-viscosity bituminous crack sealant that MoDOT has used for a number of years for crack sealing in concrete and asphalt pavements and bridge decks.

The SIMCON bonded plate alternate was chosen for this study mainly because it had the potential as a good long-term solution to the problem at hand. SIMCON plates are made by infiltrating "cement-fine sand" slurry into a dense steel-fiber mat (1/2 – 1 in. thick). The resultant high performance composite has approximately 3-5% steel fibers by volume. SIMCON has excellent structural ductility. The toughening provided by the steel fiber mat ensures distributed fine cracking instead of large localized cracking typical with cement/ploymer-based brittle composites. These fine cracks, typically not visible to the naked eye can be easily sealed using conventional methods applied for repairing concrete decks.

2.6.2 Details of the composite specimen for crack-repair tests

The specimens used in this part of the study were identical to those used in the previous fatigue tests conducted for MoDOT [2]. The specimen was made up of a 9/16-in. steel base plate of dimensions 4-in. x 15-in. Two bearing plates were welded to the bottom surface of the steel plate at the two ends. The bearing plates extended one inch past the width of the base plate on each side. Four steel rockers were used to provide end supports to the specimen at the extensions (Fig. 2.14). This allowed the composite beams to be supported without applying direct load to the wearing surface, thus prevented local damage to the

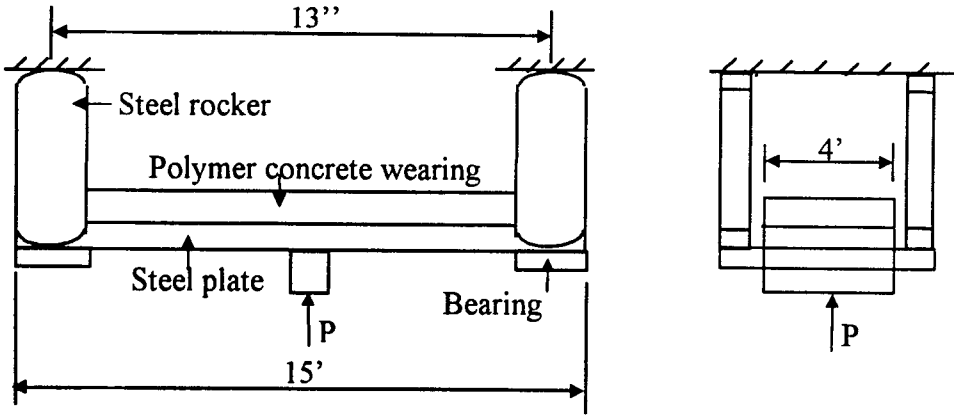

Fig. 2.14 Details of the composite steel-PC specimen

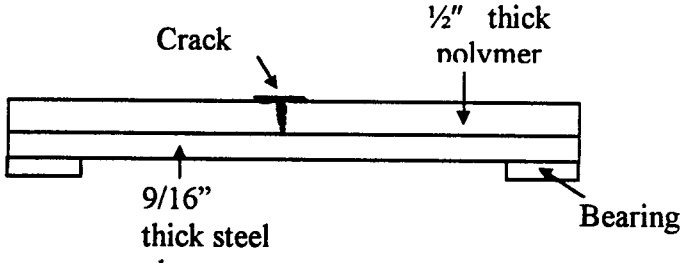

(a) Wearing surface crack repaired by Pavon / MMA sealant

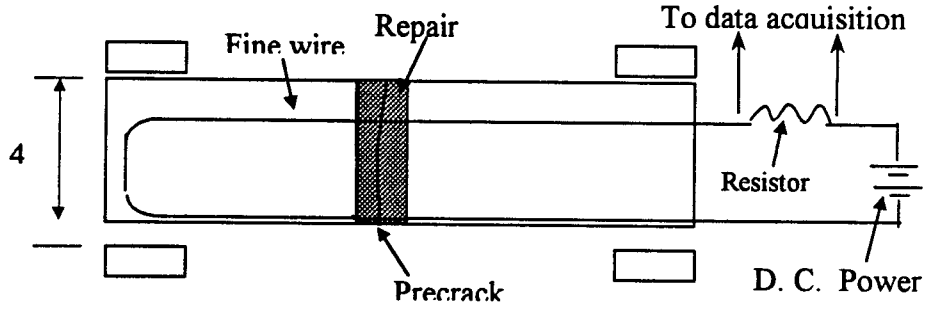

(b) Plan view of the test specimen in (a) showing wiring diagram of the crack detection system

Fig. 2.15 Steel – PC composite specimen with wearing surface crack repaired using Pavon / MMA sealant materials

wearing surface during the tests. The center to center distance between the two bearing plates was 13- in., simulating the section of the bridge deck that is centered over and loaded by a longitudinal stringer. The PC wearing surface was applied to the top surface of the plate. The thickness of the wearing surface including the broadcast aggregates on the top was approximately 1/2-in.

2.6.3 Specimen fabrication

The steel base plate was sand blasted to clean the top surface to provide good bond strength between the wearing surface and the plate. The plate was enclosed along its sides by a plastic/wood form. Rope caulking was placed in the gaps between the plate and the form to keep the epoxy from leaking out during specimen fabrication. Silicon lubricant was applied to the plastic forms to aid in the specimen demolding process. The PC mixture for the composite specimen was made using the same mix design used for plain PC specimens. The PC was placed on top of the steel plate. A table vibrator and a wooden trowel were used to compact the wearing surface and to spread the material evenly on the plate. After casting the PC, the top surface of the wearing surface was broadcast with crushed basalt aggregates to provide traction surface identical to that on the bridge deck. The composite specimens were kept at room temperature for 24 hours before demolding. The specimens were subsequently cured for an additional five days so as to allow the PC to attain its full strength. Wearing surfaces of the cured specimens were then precracked statically in flexure before applying appropriate repair procedures.

2.6.4 Precracking and crack-repair procedures

The steel-PC composite specimens were placed inside the temperature-controlled testing chamber at 20°F for three hours. The specimens were then subjected to midspan static flexural loading until cracking of the PC wearing surface occurred due to the tensile stresses from the negative bending at midspan. To ensure consistency a maximum static flexural load of 3,000 lb. was used for precracking the wearing surface.

Three different crack repair materials/procedures chosen for the investigation as described earlier in Section 2.6.1 included:

1. Transpo T-71 Methyl Methacrylate (MMA) crack sealant

2. Pavon asphalt crack sealant
3. SIMCON bondable plates.

MMA and Pavon crack sealant were used to repair two specimens each. Three composite beams were repaired using the SIMCON bondable plates. Procedures used for the repair with MMA and Pavon were somewhat similar and are described below.

Prior to repair of the wearing surface, the crack faces and surrounding area were sandblasted to clean the surfaces. Transpo MMA sealant was mixed with silica flour and sand (2:1 ratio by volume). The mixture of the repair material was then applied to the crack surfaces until excess material flowed out of the sides. A brush and a wooden applicator were used to sweep and squeegee the mixture into the crack. The repair material was also used to cover about one inch width of the surrounding wearing surface (one half inch on each side of the transverse crack) to facilitate a better seal. The Pavon asphalt crack sealant was mixed with an equal volume of water as recommended by the manufacturer. The sealant was applied in the same manner described earlier for the application of MMA. Figure 2.15 shows the schematic of the wearing surface cracks repaired using Pavon/MMA crack sealant. Figure 2.16 shows a photograph of a precracked specimen repaired by Pavon asphalt concrete.

The SIMCON bondable plate was fabricated as described here. The stainless steel fiber mat [16] was first placed into a wooden mold (inside dimension of 16-in. x 13-in. x 1-in.). The mix proportions for the cement mortar slurry was designed so that it could effectively penetrate the steel fiber mat. A previous study conducted at University of Missouri suggested that the following mix design would be suitable for this application [16]. The mix proportion used was cement:sand:water :: 1:1:0.35. Sand used passed through a #16 sieve, and 9.65 ounces of super-plasticizer was used for every 100 lb. of cement.

After mixing the above constituents thoroughly, the slurry was poured into the wooden mold containing the steel fiber mat. A table vibrator was used to consolidate the specimen. The SIMCON plate was demolded after allowing it to set for 24 hours. The plate was then cured in lime-saturated water for a period of seven days. It was then sawed into 15-in. x 4-in. x 1-in. plates, so that each SIMCON plate would cover the entire PC wearing surface of the precracked composite beam. The plate was bonded to the PC surface using FASTENAL epoxy binder. Sufficient amount of epoxy binder was applied to the wearing surface to ensure that there were no gaps between the PC and the SIMCON plate. Figures

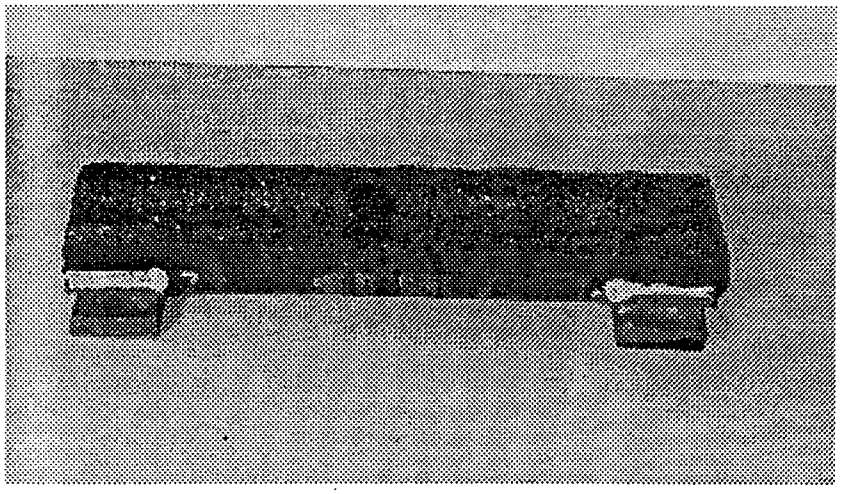

Fig. 2.16 PC wearing surface repaired by Pavon asphalt sealant

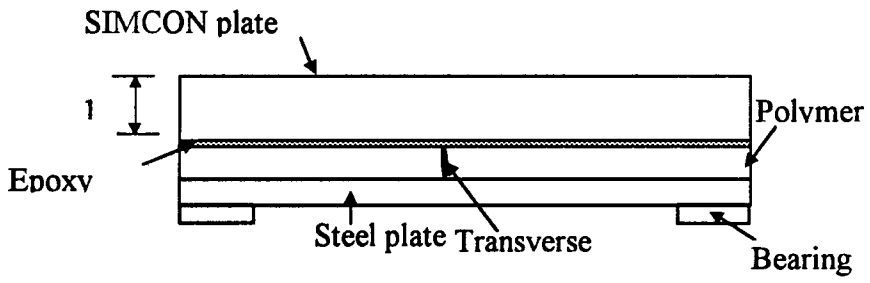

Fig. 2.17 Bonding of SIMCON plate as one potential crack repair procedure

2.17 shows a schematic of a SIMCON plate bonded to the cracked PC wearing surface specimen.

2.6.5 Crack repair tests

Steel–PC composite specimens with the repaired wearing surface cracks were subjected simultaneously to fatigue loading and temperature variation to evaluate the performance of the three repair materials/procedures. The load cells and deflection measurement devices used in the repair tests were the same as those used in the flexural tests on plain PC beams. Two specimens repaired using the same material/procedure were loaded in parallel so as to provide replicate data and to save time. Cracking of the repaired wearing surface was detected by a sudden increase in deflection accompanied by a decrease in flexural load. The stiffness of the specimen was computed by dividing the amplitude of the load by the amplitude of the deflection. The stiffness of the composite beam drifted somewhat with the test temperature. However, a clearly identifiable decrease in stiffness when the repaired wearing surface cracked again allowed detection of this type of failure.

Another technique was also concurrently used to detect the cracking of the repaired wearing surface. A 0.004 in. diameter wire was glued to the top surface of each specimen along two longitudinal edges using a rapid setting epoxy adhesive. The wire was connected to a resistor, and the wire-resistor pair was then connected to one channel of the LabVIEW data acquisition board. Crack in the wearing surface would result in a break of the electrical continuity of the crack detection system. By applying a current to the circuit, failure in the wearing surface was reflected as a drop in the voltage signal. Figure 2.15 (b) shows the wiring diagram for the crack detection set-up.

Ram displacement control was used to simulate load control in the crack repair tests. Since the wearing surface material and thickness were same for the two specimens tested simultaneously, the flexural loads applied were approximately equal if the mid-span deflections of the specimens were equal. The specimens were loaded sinusoidally at 5 Hz between the minimum and maximum loads of 150 lb. and 1,150 lb., respectively. The upper limit load of 1,150 lb. was identical to that used in the previous fatigue tests at MU [2,9]. The temperatures inside the chamber were measured using thermocouples placed at various locations. These temperature values and the time read from the computer's internal clock

were written to a data file at regular intervals. By matching the time recorded by the data acquisition computer and temperature control computer, the temperatures inside the chamber at the time of failure of the repaired wearing surface could be obtained. Each specimen was loaded until the failure of the repaired wearing surface crack occurred or until approximately two million cycles of fatigue loading were applied without failure. The performance of the specimen during the fatigue test was evaluated to study the effectiveness of the crack repair procedure for the PC wearing surface system on the Poplar Street Bridge.

2.6.6 Temperature control program

The specimens were simultaneously subjected to fatigue loading and temperature change. The temperature inside the chamber was controlled to vary cyclically to simulate the in-service temperature condition experienced by the bridge deck.

Figure 2.18 shows the variation of test temperature with respect to time. The corresponding number of fatigue loading cycles (at a loading rate of 5 Hz) is also plotted. A temperature control cycle consisted of a summer section and a winter section. Each of these sections contained two and a half daily cycles. The highest and lowest temperatures for a summer section were 165°F and 45°F, respectively. Those for a winter section were 70°F and 0°F. These temperatures were selected based on the temperature records obtained from the Lambert Airport in the St. Louis area. The specimens would experience about 2.4 million loading cycles at the end of one complete temperature control cycle. This temperature control scheme was same as that used in previous fatigue tests. Further details of the temperature control computer program are described by Rigdon [9].

2.6.7 Data acquisition program

For each of the two specimens in the parallel loading scheme, time-histories of three parameters were recorded using the LabVIEW data acquisition software. These were the flexural load, mid-span deflection and voltage across the wires used for crack detection. The load and deflection were dynamic signals in sine wave form (5 Hz). The data acquisition process (sampling rate, etc) for these dynamic signals was identical to that used in the flexural fatigue tests and described earlier in Section 2.5.3. The amplitudes and phase shifts of these signals were computed using a least square fit algorithm. The voltage across the thin

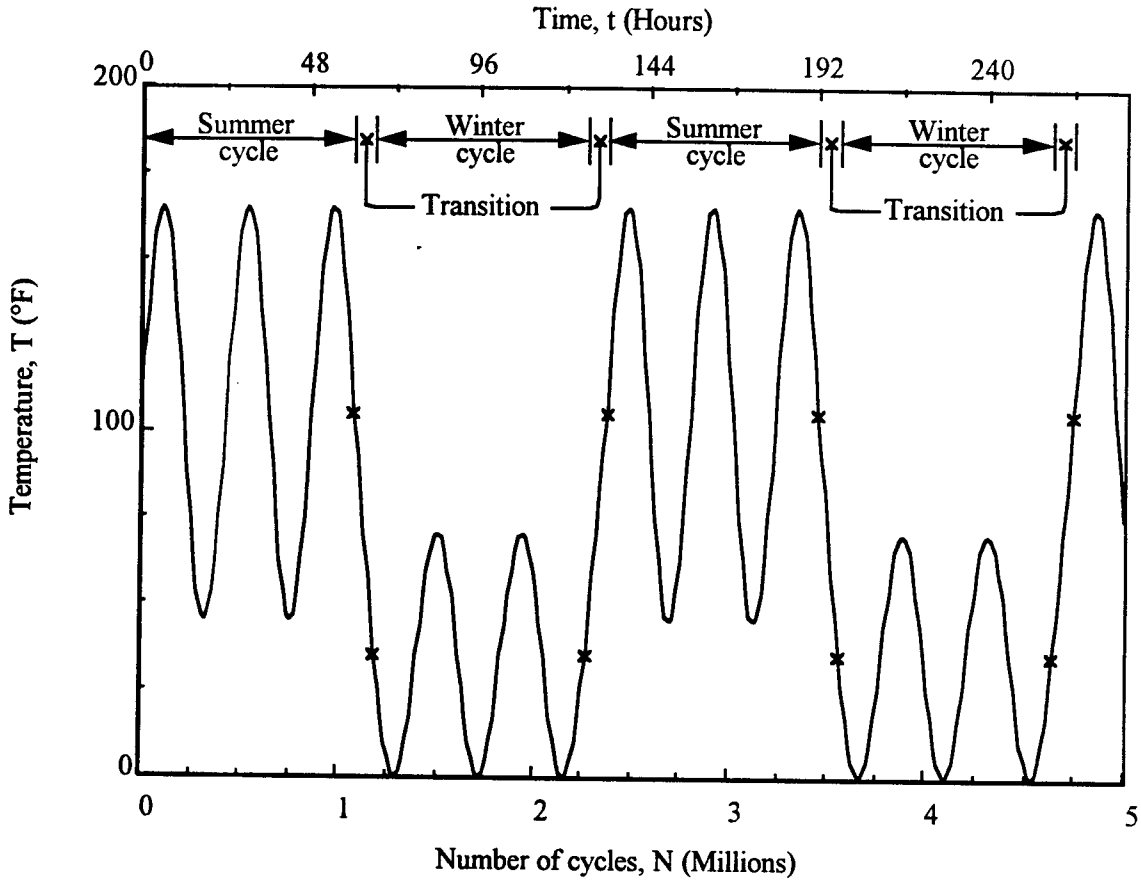

Fig. 2.18 Temperature variation versus time and loading cycles

wires was essentially a constant signal. Therefore, the average value of the fifty data points (acquired during each sampling cycle) was calculated. Real-time histories of the load and deflection responses were plotted on the computer screen, which allowed monitoring of these dynamic signals during the test. In addition, digital indicators on the LabVIEW-generated screen were used to display the amplitudes of the signals and the stiffness of each specimen. The voltage across the resistor from the crack detection set-up for each specimen was also displayed as a function of time. Newly acquired data points were appended to the chart and data file. By identifying the time when voltage in the crack detection set-up droped to zero, cracking in the repaired specimen could be instantaneously detected.

2.6.8 Evaluation of the crack repair procedures

Results from the crack repair tests are summarized in Table 2.6. Although the composite specimens with the wearing surface cracks repaired by Pavon asphalt crack sealant sustained relatively larger number of fatigue cycles before failure than those repaired by the Transpo MMA sealant, the beams repaired using either of the two materials sustained less than 5,000 cycles of fatigue loading before the repaired cracks failed again. The specimens were then taken out of the test chamber to examine the repaired cracks. All new cracks were through the thickness of the PC wearing surface, and occurred at the same locations as the original wearing surface cracks. The new cracks were much smaller compared with their original sizes, and not easily visible to the naked eye. The cracked beams were then tested under cyclic loading for additional three hours (approximately 54,000 fatigue cycles) to evaluate the growth of cracks. No appreciable increases in the width of these cracks were observed due to the additional loading cycles.

The test results indicate that both the Transpo MMA and Pavon asphalt sealant can be used to seal the cracks on the PC wearing surface, and significantly reduce the sizes of the cracks. This would result in minimizing the potential for infiltration of water and deicing salt into the deck surface. However, the wearing surface cracks repaired using both materials are expected to reflect through on the surface after a very short period of exposure to normal traffic. This is partially because once epoxy cures, it does not bond well with subsequent layers of the repair material(s). One has to rely on mechanical interlock to transfer loads from the newly placed material to the original cracked epoxy concrete wearing

Table 2.6 Results from the crack repair tests on steel – polymer concrete composite specimens

Specimen number	Repair technique	Number of cycles to failure
1	Transpo T-71 MMA sealant[1]	1,260
2	Transpo T-71 MMA sealant[1]	30
1	Pavon asphalt sealant[1]	4,860
2	Pavon asphalt sealant[1]	2,460
1	SIMCON fiber reinforced concrete[1]	≈180,000 [2]
2	SIMCON fiber reinforced concrete[1]	> 1,730,000
3	SIMCON fiber reinforced concrete[1]	> 1,730,000
2	SIMCON fiber reinforced concrete[3]	≈ 471,600
3	SIMCON fiber reinforced concrete[3]	> 1,730,000

1. Specimen tested under the maximum fatigue load of 1,150 lb.
2. Specimen failed due to the delamination of the fiber reinforced concrete plate from the polymer concrete surface caused by the failure of the FASTENAL epoxy binder at high temperature.
3. Specimen tested under the maximum fatigue load of 3,500 lb.

surface. This makes crack maintenance of a polymer concrete wearing surface difficult.

It was observed from the repair tests that the Pavon asphalt sealant had excellent ability to penetrate small cracks. More Pavon material was consumed compared to Transpo MMA sealant to repair wearing surface cracks of similar width indicating a more complete infiltration of the crack. The MMA material was relatively more viscous, and could not fully infiltrate very fine cracks. The MMA material commenced hardening in about ten minutes with the addition of a recommended catalyst. The Pavon asphalt sealant took about one hour to become tacky. From a practical standpoint too, it is easier to apply Pavon compared to the MMA material.

The bonding of SIMCON plate, one of the potential wearing surface repair procedure, significantly increases the stiffness of the bridge deck system. Consequently, for proper comparison of results with those from the other two crack repair procedures, one would have to choose between applying comparable maximum fatigue load or applying comparable maximum deflection level. The two cases represent two limiting situations as far as the mechanical performance of the bridge deck system is concerned.

The first type of fatigue test used three composite specimens repaired using bonded SIMCON plates that were subjected to the fatigue loading cycles from 150 lb. to 1,150 lb. (same loading range used for Pavon and MMA repaired specimens). This resulted in significantly smaller tensile stress magnitudes in the top fiber of the SIMCON plate (228 psi versus 1,171 psi for the two other repair procedures) as a result of the increased stiffness and change in the location of the neutral axis. In this type of test, one of the three composite specimens failed after being subjected to the fatigue loading and high temperatures (from 100°F to 165°F) for approximately 10 hours ($\approx$ 180,000 loading cycles). The failure was due to the debonding of the SIMCON plate from the PC wearing surface. The FASTENAL epoxy binder used to bond the SIMCON to the PC failed on exposure to the high temperatures, and thus caused separation at the interface (Fig. 2.17). The other two specimens repaired by the SIMCON plate were thus only tested under cold temperature exposure, ranging from 0°F to 70°F, to evaluate the performance of the repair procedure (most severe case of mechanical plus thermal loading). These two specimens performed very well in the fatigue test. Both beams sustained fatigue loading cycles for 96 hours ($> 1{,}73 \times 10^6$ loading cycles) without any apparent failures.

After the test was stopped, the specimens were taken out from the temperature chamber for examination. No cracks were observed on the surface of the SIMCON plate. No delaminations at the interfaces between the SIMCON/PC or PC/steel were observed.

In the second type of test on SIMCON repaired specimens, maximum deflection level identical to that of the two earlier repair procedures was used. The two specimens that survived the first type of test were subsequently tested by using the same mid-span deflection value as that used in the previous tests on steel-PC composite beams repaired by Pavon and MMA. This type of loading subjected the specimens to a maximum fatigue load of approximately 3,500 lb. The minimum load and loading frequency remained the same as those used in the previous tests. The SIMCON plates in this second type of test were subjected to a maximum tensile stress of 694 psi at mid-span.

One of the two specimens cracked after being subjected to fatigue loading at cold temperature range (0°F to 70°F) for about 26.2 hours (471,600 loading cycles). The beam failed by the formation of a single transverse vertical crack through the thickness of the fiber reinforced concrete and PC layers. This crack occurred at a location different from the original crack in PC wearing surface. The other beam sustained fatigue loading at this level for 96 hours ($> 1{,}73 \times 10^6$ loading cycles) without cracking or delamination failures at the time the test was stopped.

Based on the limited tests conducted in this study, it appears that repairing the cracks in the PC wearing surface using SIMCON plate bonding holds good promise. Increases in dead load of the bridge due to the wearing surface as well as increase in deck stiffness are some obvious drawbacks with this repair approach. However, long-term maintenance becomes relatively easy and the potential extension of life of the wearing surface is expected to be far superior to that provided by the other two repair procedures.

CHAPTER 3 – WEARING SURFACE STRESS ANALYSIS

3.1 Scope and motivations

One of the original objectives of the analytical component of this study was to investigate reasons for the occurrence of the two initial transverse wearing surface cracks in the thickness transition zones at the two ends of the rightmost eastbound traffic Lane E4 (Fig. 1.6). It was later extended to analyze other transverse cracks in the thickness zone of the eastbound lanes as well as longitudinal fatigue cracks over stiffeners observed in the more recent inspections, Figs. 1.7-1.9 [8]. Given the complicated structural geometry of the bridge deck system and the temperature and strain-rate dependent response of the wearing surface material, it will only be possible to include approximate analysis methods on the idealized structure in this investigation. Results from the analysis presented here while qualitatively helpful to understand the nature of cracks observed on the wearing surface, should not be used for absolute quantitative interpretations because of the idealizations in the structural geometry as well as the material properties of the PC wearing surface. Analysis aspects presented in this chapter includes the computation of thermal stresses in PC caused by the mismatch in coefficients of thermal expansion between steel deck and PC wearing surface, and by the difference in thermal expansions between the two webs of the rightmost box girder. The tensile stresses in PC wearing surface induced by traffic load is also computed using the orthotropic bridge deck theory to interpret the cause of the longitudinal fatigue cracks in the wearing surface. While reasons for the presence of longitudinal fatigue cracks could likely be explained from an earlier idealized analysis [2], transverse cracks in the thickness transition zone of the eastbound lanes on the wearing surface was not originally anticipated.

3.2 Possible reasons for transverse cracks in the wearing surface

The presence of transverse cracks in the thickness transition zone of the eastbound lanes can be attributed to a combination of reasons.

1. The PC wearing surface and steel deck have different coefficients of thermal expansion and modulus of elasticity. A uniform temperature variation would cause one material to expand or contract more than the other. Normal stresses and

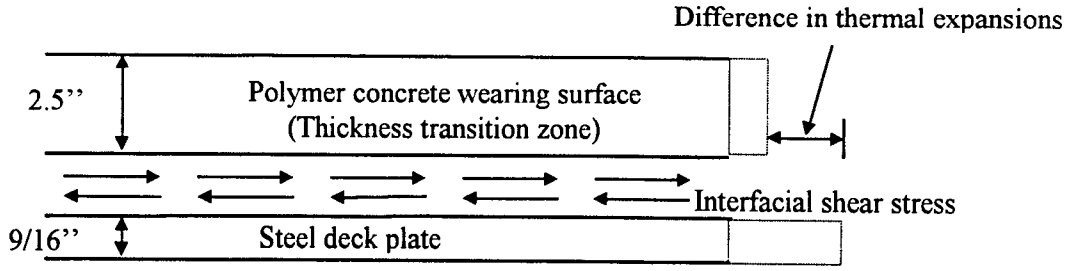

Fig. 3.1. Thermally induced interfacial stresses

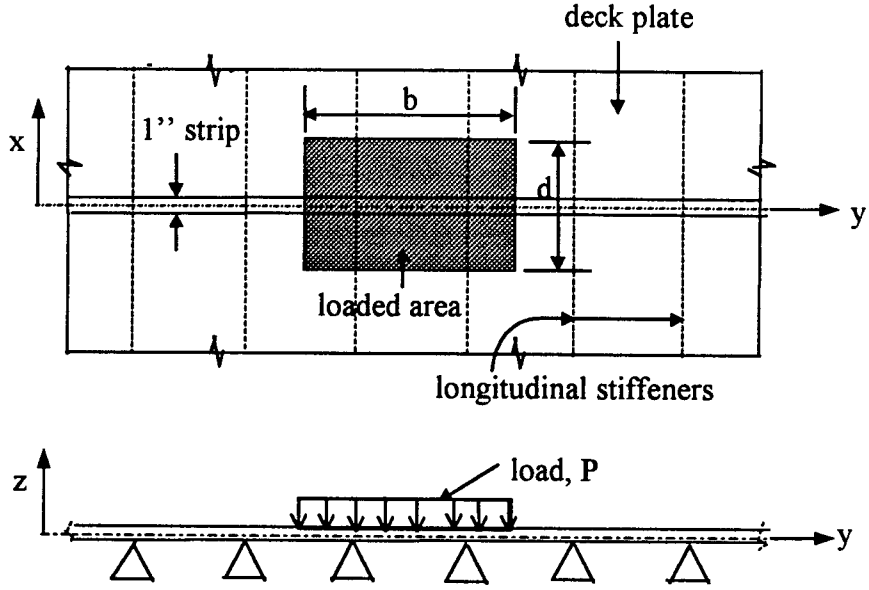

Fig. 3.2. Bridge deck plate treated as continuous beam supported on stiffeners

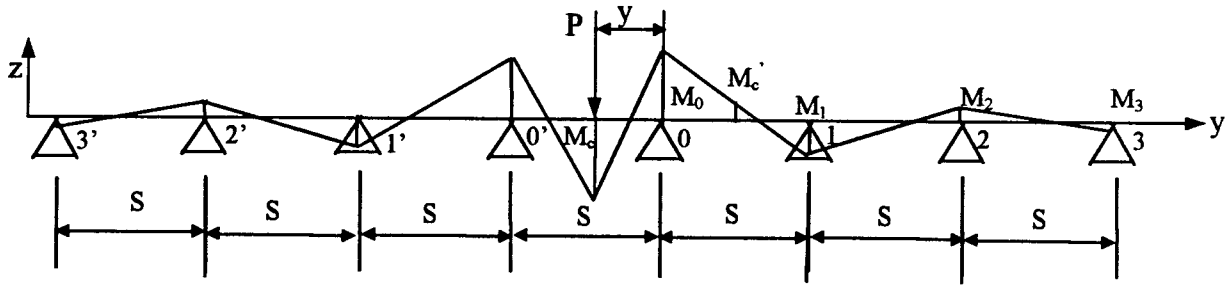

Fig. 3.3. Bending moments of a continuous beam due to a concentrated load

interfacial shear stresses are then developed in both materials as a result. These thermally induced stresses can cause tensile cracking in the PC wearing surface and/or result in the delamination of the wearing surface at the interface. Figure 3.1 shows thermally induced interfacial stresses.

2. Differential thermal expansion between the two webs of the south box girder (which supports the eastbound bridge deck carrying Lane E4, Fig. 1.6) due to non-uniform heating or cooling during the day can result in cracks in the wearing surface. The temperature variation on the outside web, which is exposed directly to the sunlight, causes significant expansion (and subsequent contraction). The inside web however, is not exposed to direct sunlight. The PC wearing surface above that box girder can consequently be subjected to tensile stresses resulting from the difference in thermal expansions between its two webs as shown later in this chapter.

3. The Poplar Street Bridge in Saint Louis experiences significant daily and seasonal temperature changes. Based on the experimental results, the mechanical properties of the Transpo T-48 PC material are sensitive to test temperatures. The PC wearing surface exhibits brittle behavior at cold temperatures. The orthotropic steel deck of the Poplar Street Bridge is subjected to large deflections (3 to 4 in. of deflection is common during normal peak-traffic periods) due to the flexible structural characteristics of such decks. The limited strain capacity of PC at cold temperatures, is as a result, of concern with regard to potential for cracking.

4. The two earliest transverse cracks in the wearing surface being studied initiated at locations very close to the top of the inside web of the south box girder of the eastbound bridge. The bridge deck is stiffened in the longitudinal direction by stiffeners and the box girders that run along the length of the bridge. However, the box girder webs provide much stiffer support to the deck plate than the trapezoid stiffeners. As the result, the wearing surface immediately above the box girder webs is subjected to a relatively larger magnitude of negative bending moment. This may also contribute to the tensile cracking at these locations.

3.3 Stresses in the PC wearing surface due to traffic loads

The analysis presented in this section provides an explanation for the longitudinal fatigue cracks observed in the wearing surface during the recent few field inspections [8].

3.3.1 Wheel load and loaded area dimensions

The following derivation of the stresses in the orthotropic steel deck plate due to traffic load is based on the procedures recommended in the AISC's "Design Manual for Orthotropic Steel Plate Deck Bridges" [1]. The deck plate supported on the longitudinal stiffeners is treated as a 1-in. wide beam continuous in the transverse direction over the ribs acting as rigid supports. Figure 3.2 shows the loaded area and coordinate system for the bridge deck. The maximum allowable axle load for a truck is 24 kips based on the AASHTO specifications. The wheel load, P, applied on top of the steel deck plate at each side of the axle is 12 kips. This wheel load is carried by two truck wheels, and distributed on the loaded area of dimension b x d. The track width (in the transverse direction of the deck plate), b, is 22 in. for the 12 kips dual tires. The length of the deck plate in the longitudinal direction involved in bearing the wheel load, d, is 12 in. Therefore, the unit pressure, p, at the loaded area, including 30% impact factor, is computed as 59 psi.

3.3.2 The concept of influence line

Figure 3.3 shows a continuous beam of a constant section modulus supported over evenly spaced rigid supports. Panel 0-0' is subjected to a concentrated load, P. The resulting bending moments in unloaded panels decrease in magnitude with a constant carry-over coefficient, κ. If M_0 is the bending moment at the support 0, then the moments at supports 1 and 2, M_1 and M_2, are κM_0 and $\kappa^2 M_0$, respectively.

The value of κ was derived by applying three-moment equation for the unloaded beam

$$M_0 + 4M_1 + M_2 = 0 \qquad (3.1)$$

Substituting the expressions for M_1 and M_2, yields $\kappa = -0.2679$. Using this carry-over coefficient, the bending moments at the support and mid-span of stiffeners are hence computed by means of influence lines.

"Design Manual" [1] derived the equations of the influence line for the bending moment at support 0, M_0, and the moment at the mid-span of the Panel 0-0', M_c, as follows:

$$\left(\frac{M_0}{SP}\right) = (-0.5)\left(\frac{y}{S}\right) + 0.866\left(\frac{y}{S}\right)^2 - 0.366\left(\frac{y}{S}\right)^3 \quad (3.2)$$

$$\left(\frac{M_c}{SP}\right) = 0.183\left(\frac{y}{S}\right) + 0.317\left(\frac{y}{S}\right)^2 \quad (3.3)$$

where y is the distance between the concentrated load position and Support 0, and S is the distance between the webs of the stiffeners for the Poplar Street Bridge which is 13 in.

The equation of the influence line for the bending moment at the mid-span of the distant Panel 0-1, M'_c, is:

$$\left(\frac{M'_c}{SP}\right) = -0.183\left(\frac{y}{S}\right) + 0.317\left(\frac{y}{S}\right)^2 - 0.134\left(\frac{y}{S}\right)^3 \quad (3.4)$$

3.3.3 Analysis of bending moments in the deck plate

The bending moments in the deck plate at the support of a stiffener and at the mid-span between webs of the stiffeners are calculated using the following dimensions and properties: The plate thickness is 9/16 in., and webs of the stiffeners are spaced at 13 in. The deck plate is subjected to a 12 kip wheel load distributed over the dimensions b x d = 22-in. x 12-in. The unit pressure, p, is 59 psi.

Figure 3.4 shows the deck plate treated as a continuous beam supported over the webs of the stiffeners, and the loading position of the plate. Bending moment at Support 0 is computed by integration of Eq. 3.2. over Panel 0-1 and Panel 0-0' (for a total distance y of 22 in.). The concentrated load P in the equation is replaced by "pdy". The moment over the stiffener as obtained from this computation, M_0, is −1,019 lb-in.

Figure 3.5 shows the loading position of the deck plate in the computation of the bending moment at the mid-span between Panel 0-0'. The moment is computed by integrating Eq. 3.3 (for a distance y of 13 in. which is the distance between the two webs of the stiffener) and Eq. 3.4 (for a distance y of 4.5 in. beyond each web of the stiffener). The concentrated load P in both equations is again replaced by "pdy". The bending moment at the mid-span, M_c, is computed as 580 lb-in.

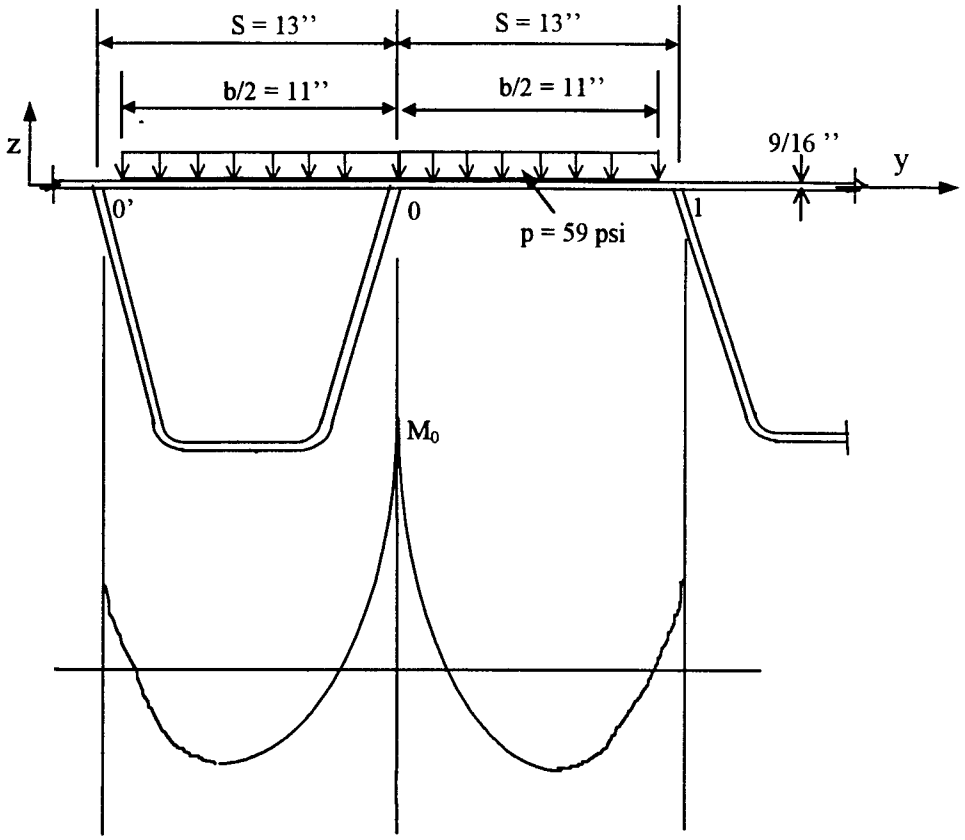

Fig. 3.4. Bending moment at support

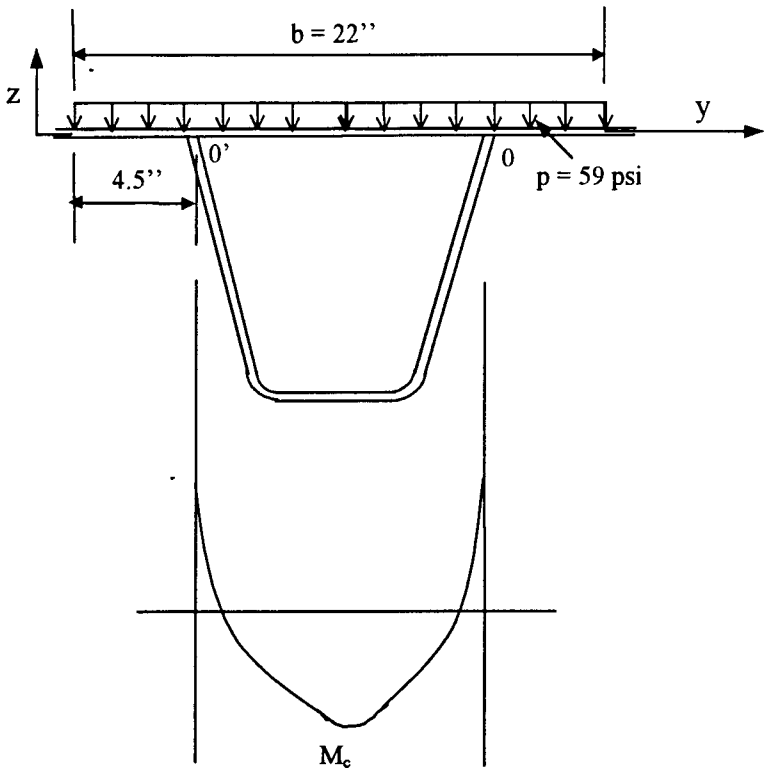

Fig. 3.5. Bending moment at mid-span

The above computation was performed by treating the full deck plate as a 1-in. wide continuous beam supported over the webs of the longitudinal stiffeners. The results of the analysis showed that the maximum bending moment in the continuous beam occurs above the webs of the stiffeners, the value of the moment is –1,019 lb-in.

Considering the contribution of the longitudinal direction of the full deck plate in bearing the traffic load, the bending moment (over the stiffener webs) in the transverse direction of the full deck plate is smaller than the moment (over the supports) in the continuous beam of 1-in.width. "Design Manual"[1] introduces the concept of plate factor, ψ, defined as the ratio between the bending moment in the transverse direction of the full deck plate, to the corresponding moment in the continuous beam of unit width to account for this fact. The value of plate factor depends on the ratio of the width of the loaded area to the span of the beam, d/S. With the ratio d/S = 12/13 = 0.923 as used in this study, the plate factor is specified as 0.85. The negative bending moment in the full plate at the support, M_0, is thus reduced from –1,019 lb-in. to – 866 lb-in.

3.3.4. Analysis of stresses in the wearing surface

The maximum negative bending moment occurs in the deck plate over webs of the stiffeners. The tensile stress in the top fiber of the PC wearing surface is computed by dividing the moment by the section modulus of the PC - steel deck composite plate. The following dimensions and material properties are used in the analysis:

The thickness of steel plate, t_s, is 9/16 in., and the width is 1-in. The thickness of the wearing surface, t_{pc}, is 3/8 in. in the main lane area (outside of the transition zones). The modular ratio between the steel deck and the PC wearing surface, n, is 29 when the temperature of PC is from 100°F to 165°F, and 14.5 when the temperature of PC is from 0°F to 35°F, as determined in the flexural fatigue tests conducted by Rigdon [9]. The section modulus of the top fiber of PC, S_{top}, can thus be computed as 0.798 in^3 (n = 29) and 0.469 in^3 (n = 14.5). Using the bending moment of – 866 lb-in, tensile stress in the top surface of the PC over the stiffeners, σ_y, is obtained as 1,846 psi and 1,085 psi for n equals 14.5 and 29, respectively.

Using the peak strain in the deck plate measured in the earlier field strain measurements [10], the maximum in-service tensile stresses in the wearing surface over webs

of stiffeners were computed as 1,895 psi and 995 psi for a modular ratio, n, equals 14.5 and 29 respectively. These stress values agree very well with the maximum tensile stresses in PC computed using orthotropic bridge deck theory in this study. As discussed by Cao [8], the PC wearing surface could endure about 5,236 fatigue loading applications of the maximum tensile stress (995 psi) at high temperature (100°F – 165°F) before cracking. However, at cold temperature (0°F – 35°F), the PC wearing surface would crack after only 2,851 fatigue loading applications of the maximum stress (1,895 psi). This analysis shows that the combination of cold temperature and fatigue traffic loading is detrimental to the PC wearing surface. This is likely to be the primary reason for the longitudinal tensile cracking on the PC wearing surface over the webs of the stiffeners and box girders which were first observed in September 1996 (after about four years of service of the PC wearing surface).

3.4 Computation of thermally induced stresses in the PC wearing surface

The analysis presented in this section provides an explanation for the transverse wearing surface cracks observed in the thickness transition zones of the rightmost eastbound Lane E4.

The Poplar Street Bridge consists of two independent bridges. Each of the bridges is supported in the longitudinal direction by two box girders. Because the outside web of the south box girder of the eastbound bridge is exposed directly to the sunlight, it is subjected to fairly significant thermal expansion/contraction due to the daily and seasonal temperature changes. However, since all other box girders as well as the inside web of the south girder of the eastbound bridge are shielded from direct sunlight, the thermal expansions (and subsequent contractions) of the webs of those box girders are relatively negligible. The distance between the two webs of a box girder is 5 ft. 5in. The transverse supports for the bridge deck are provided by floor beams which are widely spaced at 15-ft. centers. Given the normal rates of changes in temperature of the outside web and the relatively long duration for achieving steady state, it is reasonable to assume that there is significant variation in temperature between the outside and inside web of the south box girder. Also, the steel deck plate and the PC wearing surface have different coefficients of thermal expansion and elastic modulus. When the Steel deck-PC composite system is subjected to uniform heating or cooling, the steel deck expands or contracts more than the PC wearing surface. Therefore, the

tensile stresses in the PC wearing surface would be produced as a result of the differential thermal expansion between the two box girder webs, and the differences in coefficients of thermal expansion and elastic modulus between the two materials. These thermally induced stresses can contribute to the transverse tensile cracking on the PC wearing surface at the two end regions of the rightmost Lane E4 which is supported by the south box girder of the eastbound bridge.

Due to the complicated structural geometry of the bridge deck system, it has only been possible to include approximate analysis methods using an idealized structural model in this study. Analysis incorporates the influence of temperature, bridge deck geometry, and materials properties in the computation of the thermally induced stresses in the composite deck. Even a more detailed numerical model using the finite element analysis would require sufficient idealizations, and thus may not significantly improve the stress solutions obtained from the simple model presented here.

3.4.1 Idealized structural model for thermal stress analysis

In this analysis, the bridge deck–wearing surface system is simplified into a structural model of a flat PC plate with a thickness, t_{pc}, of 3/8 in. (same as the thickness of PC wearing surface outside of transition zones) bonded perfectly to the top surface of a steel plate with a thickness, t_s, of 9/16 in. (same as the thickness of steel deck). The width of the composite plate is 5 ft. 5 in., same as the distance between the two webs of a typical box girder. Figure 3.6 shows the idealized model and the associated coordinate system.

The C.O.T.E. for the Transpo T-48 PC, α_{pc}, is assumed to be 9.5 x 10^{-6} in./in./°C in the following computations. The Coefficient of Thermal Expansion for the steel, α_s, was assumed to be 12.53 x 10^{-6} in./in./°C. The modulus of elasticity for steel, E_s, is 29 x10^6 psi, and the modulus for PC, E_{pc}, is 1 x 10^6 psi when the temperature of the material is from 100°F to 165°F (computed using a modular ratio between steel and PC of 29 [9]).

To simulate the influence of the differential thermal expansion between the two webs of the south box girder on the expansion of the steel deck, the temperature change for the bottom steel plate in this model, $T_2 - T_1$, is assumed to vary linearly along the width of the composite plate (Fig. 3.6). The maximum temperature variation along the width (y axis) of the steel plate occurs at the location y = 0 (above the outside web of the box girder). The

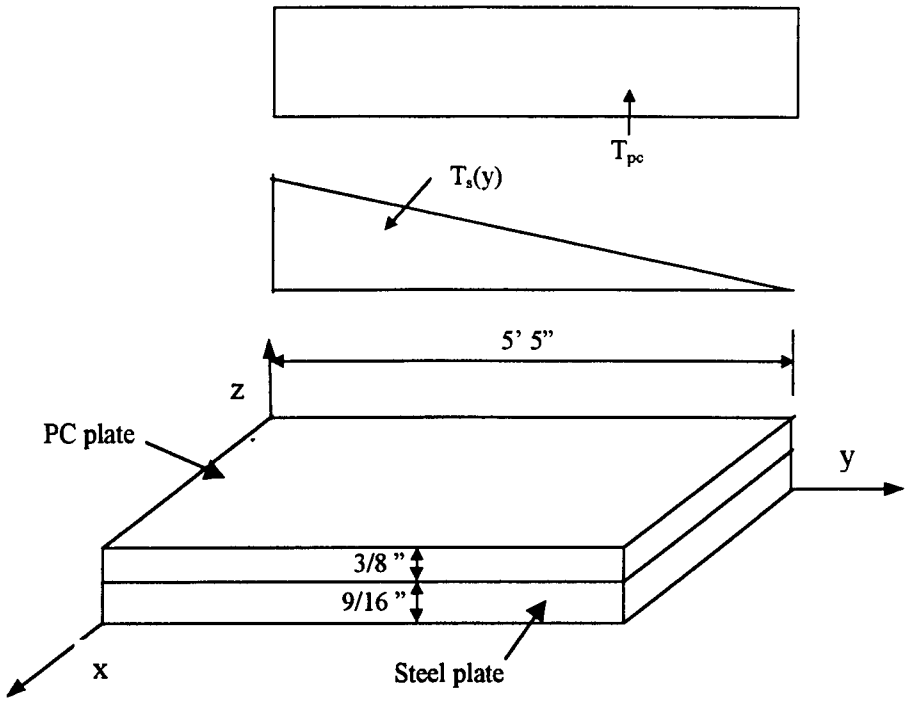

Fig. 3.6. Composite plate and temperature variation for thermal analysis

initial temperature at this location, T_1, is selected as 45°F (7.22°C), and T_2 is chosen to be 165°F (73.89 °C). This temperature variation represents the typical daily temperature change on the bridge deck during the summer season (nighttime deck temperature to peak daytime deck temperature). It is assumed that there is no temperature variation on the other side of the steel plate (at the location y = 65 in., above the inside web of the box girder). Since the black PC wearing surface is exposed to direct sunlight, the top PC plate is assumed to be subjected to a uniform temperature increase from 45°F (7.22°C) to 165°F (73.89°C) along the entire width of the plate. No variations in temperature in the x and z directions are considered for both the steel and PC layers of the composite deck.

3.4.2 Analysis of stresses in the composite strip

To compute the thermal stresses in the PC, first extract a 1 in. composite strip along the width of the plate (y axis). Since the width of the strip is very small compared with the total width of 5 ft. 5 in., it can be assumed that the temperature changes are uniform in both the PC and steel strips.

The following analysis of thermal stress is based on the investigation of Timoshenko [17]. This theory was initialy developed to compute the stresses in bi-metal strip thermostats subjected to uniform temperature change. The derivation is based on the flexural behavior of a composite beam. The following assumptions were made in this analysis:

1. The C.O.T.E. for both materials remain constant and are not functions of temperature.
2. The composite strip is not subjected to additional external forces (thermal loading is considered independent of mechanical loading).
3. Both steel and PC behavior in a linear elastic fashion.
4. Cross-sections of the beam remain planar and perpendicular to neutral axis during bending.

Figure 3.7 (a) shows that the composite beam is straight at initial temperature T_1. Fig. 3.7(b) indicates that if the composite plate is uniformly heated, the bottom layer of steel expands more than the top layer of PC. The resulting deflection of the composite beam will be concave up, as shown in Fig. 3.7(c). Forces are then produced in the top and bottom layers to maintain equilibrium and compatibility of both layers at the interface. For the steel layer on the convex side, the forces acting on the cross-section can be represented by an axial

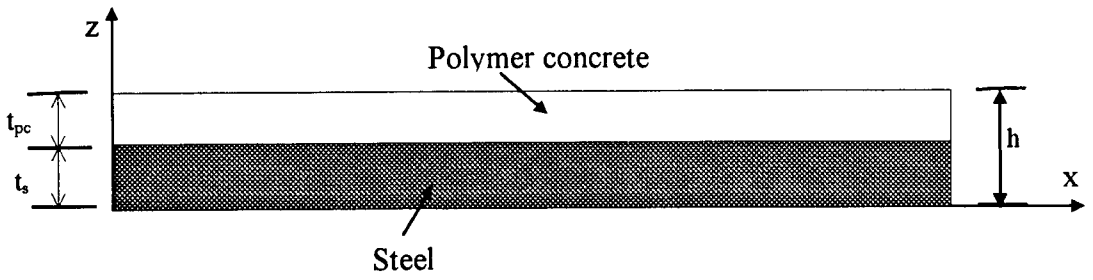

(a) Steel plate - PC composite beam

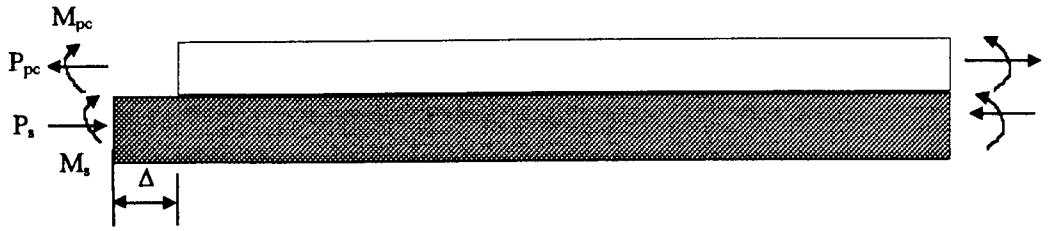

(b) Different thermal expansions during heating

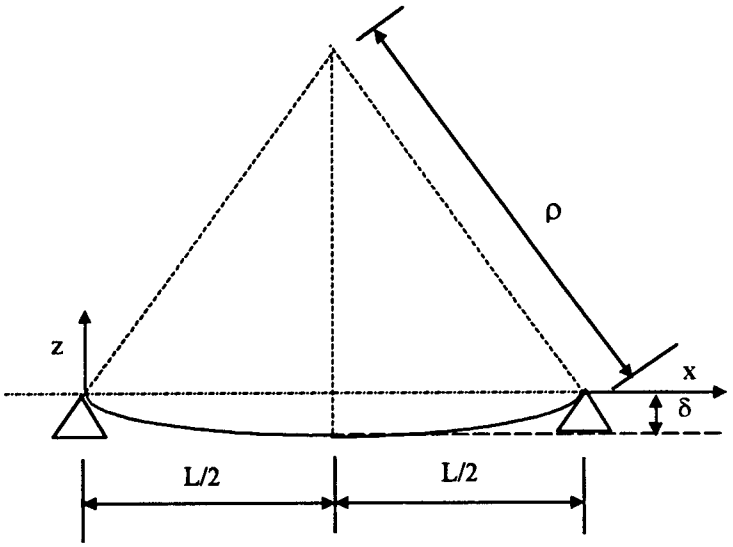

(c) Deflection of the beam

Fig. 3.7. Forces in composite beam due to differential thermal expansion

compressive force P_s, and the bending moment M_s. Forces acting on the section of PC on the concave side consist of an axial tensile force P_{pc}, and the moment M_{pc}. Considering the fact there are no external forces acting on the beam, all forces acting over any cross-section of the beam must be in equilibrium, therefore:

$$P_{pc} = - P_s = P \tag{3.5}$$

$$P\ (h/2) = M_{pc} + M_s \tag{3.6}$$

Letting ρ be the radius of curvature of the deflected beam, $E_{pc}I_{pc}$ and E_sI_s be the flexural rigidity of PC and steel, respectively, then

$$M_{pc} = E_{pc}I_{pc} / \rho \tag{3.7}$$

$$M_s = E_sI_s / \rho \tag{3.8}$$

Substituting Eqs. (3.7) and (3.8) into Eq. (3.6)

$$P\ (h/2) = (E_{pc}I_{pc} + E_sI_s) / \rho \tag{3.9}$$

Treating each layer as elastic and homogeneous, and substituting relevant material and geometry data in Eq. 3.9 gives

$$P = 9.27 \times 10^5 / \rho \tag{3.10}$$

Based on the previous assumptions, the temperature variation along the width of steel plate, $T_s = T_2 - T_1$, is a function of y, and temperature variation in PC plate, T_{pc}, remains constant along the y direction as $T_{pc} = 73.89 - 7.22 = 66.67°$. Considering that the unit elongation of the longitudinal fibers of PC and Steel must be equal at the interface, therefore:

$$\alpha_{pc}\ T_{pc} + P_{pc} / E_{pc}t_{pc} + t_{pc} / 2\rho = \alpha_s\ T_s\ (y) + P_s / E_st_s - t_s / 2\rho \tag{3.11}$$

where $t_{pc} / 2\rho$ ($t_s / 2\rho$) is the difference in unit elongation between the longitudinal fiber of PC (steel) at the center of the PC (steel) plate and the fiber of PC (steel) at the interface.

The thickness of PC plate, t_{pc}, is 3/8 in., the thickness of the steel plate, t_s, is 9/16 in. The elastic modulus of PC, E_{pc}, is 1×10^6 psi, the elastic modulus of steel, E_s, is 29×10^6 psi. The C.O.T.E. for PC, α_{pc}, is 9.5×10^{-6} psi, and the C.O.T.E. for steel, α_s, is 12.53×10^{-6} psi. Substituting these parameters into Eqs 3.5, 3.10 and 3.11, and solving for ρ yields:

$$1/\rho = [4.18 \times 10^{-6}\ T_s(y) - 2.11 \times 10^{-4}]\ \text{in.}^{-1} \tag{3.12}$$

Substituting the value of $1/\rho$ into Eqs. 3.7 and 3.10 gives

$$M_{pc} = E_{pc}I_{pc} / \rho = [1.837 \times 10^{-2}\ T_s(y) - 0.927]\ \text{lb-in.} \quad (3.13)$$

$$P = P_{pc} = 9.27 \times 10^{5} / \rho = [3.875\ T_s(y) - 195.597]\ \text{lb} \quad (3.14)$$

Where the moment of inertia for PC strip

$$I_{pc} = t_{pc}^3/12 = 0.004395\ \text{in}^4 \quad (3.15)$$

The internal normal stresses in the PC wearing surface due to differential thermal expansion between the two materials can be calculated using elastic theory for beam analysis as

$$\sigma_{x1} = P / t_{pc} - M_{pc}\,(t_{pc}/2) / I_{pc} = [9.56\ T_s(y) - 482.04]\ \text{psi} \quad (3.16)$$

$$\sigma_{x2} = P / t_{pc} + M_{pc}\,(t_{pc}/2) / I_{pc} = [11.12\ T_s(y) - 561.14]\ \text{psi} \quad (3.17)$$

where σ_{x1} denotes the stress in the top fiber of PC, and σ_{x2} is the stress in PC at the interface (Fig. 3.8).

Since the thermal stresses vary linearly through the thickness of PC plate, the resultant in-plane force per inch width, N_x, may be computed as follows:

$$N_x = [(\sigma_{x1} + \sigma_{x2}) \times 3/8] / 2 = [3.878\ T_s\,(y) - 195.596]\ \text{lb.} \quad (3.18)$$

The variation of temperature change along the entire width of the steel base plate, $T_s(y)$, can be expressed using the following linear equation:

$$T_s\,(y) = 66.67\,(1 - y / 65) \quad (3.19)$$

The resultant in-plane force and bending moment at the edge of the PC plate also cause stresses in the PC. The thermal stresses in PC at the interface far away from the edge can thus be computed as the summation of three components as

$$\sigma_x = [11.12\ T_s(y) - 561.14] + \frac{1}{65(3/8)} \int_0^{65} [3.878\ T_s\,(y) - 195.596]\,dy + \frac{y}{I_z} \int_0^{65} [3.878\ T_s\,(y) - 195.596]\,y\,dy \quad (3.20)$$

The moment of inertia of the section of the PC plate (in y-z plane) with respect to z axis

$$I_z = \frac{(3/8)(65^3)}{12} + (3/8)\ 65\ (32.5^2) = 34{,}328\ \text{in}^3 \quad (3.21)$$

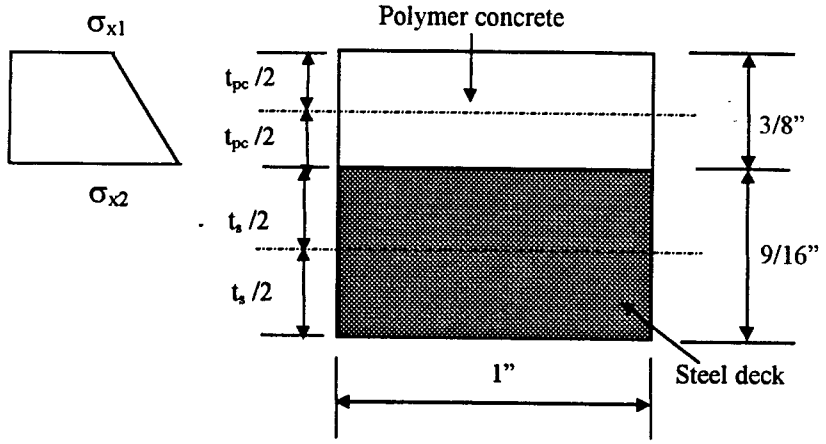

Fig. 3.8. Thermally induced stresses in polymer concrete

Substituting $T_s(y)$ (Eq. 3.19) and I_z into Eq. 3.20, it can be found that the maximum magnitude of stress in the PC plate occurs at y = 65 in. at the interface between steel plate and PC as

$$\sigma_{max} = - 1{,}175 \text{ psi} \tag{3.22}$$

Based on the above computations, when the steel plate is heated from T_1 to T_2 (T_2 - T_1 varying along the width of the plate), and PC plate is heated from 45°F to 165°F, a maximum compressive stress of the magnitude of 1,175 psi would occur in the PC plate at the location y = 65 in. (PC wearing surface over the inside web of the south box girder). It is obvious that when the temperature change experienced by the composite plate is reversed (cooled from T_2 to T_1 in steel plate, and from 165°F to 45°F in PC plate), the PC would be subjected to a maximum tensile stress of 1,175 psi at the same location. This thermally induced tensile stress is in the x direction of the composite plate (longitudinal direction of the bridge deck) as shown in Fig. 3.6.

Based on the results obtained from the previous fatigue tests on PC-Steel plate composite specimens [9], the maximum tensile stress sustained by the PC wearing surface at the time of fatigue cracking was only 1,375 psi when the material was hot (100°F to 165°F). In colder temperature range (45°F – 100°F) of the entire temperature range of interest for the above analysis (45°F – 165°F), the modulus of PC is expected to be significantly higher than 1×10^6 psi which is used in the computation, and thus is likely to produce wearing surface stresses in excess of 1,175 psi computed here. Additionally, given the idealizations made in the analysis where the structural restraints are significantly lesser than the actual structure, it is highly probable that the actual stresses in the PC exceed the failure stress of 1,375 psi required to explain the transverse cracks. The above analysis also provides an explanation for the fact that the transverse cracks originated at locations above the inside web of the south box girder where the maximum tensile stresses in the wearing surface along the transverse section of the bridge deck are expected to occur. Even while the analyses presented in Section 3.4 is based on a significantly idealized model of the portion of the bridge, it adequately demonstrates that transverse cracks can indeed develop in the PC wearing surface due largely to differential thermal expansion in the south box girder.

CHAPTER 4 - CONCLUSIONS AND RECOMMENDATIONS

4.1 Conclusions

1. The test temperature had significant influence on the mechanical properties of Transpo T – 48 PC. The modulus of elasticity, flexural strength and compressive strength of PC increased, and the failure strain decreased when the test temperature was decreased.
2. Based on the results from the static flexural tests on PC at 73°F, the load-deflection response of PC beams exhibited both linear and non-linear regions, similar to the behavior of conventional cement concrete. At 20°F, the beams exhibited a stiff behavior, and the load-deflection response was essentially linear up to the ultimate load. The beams tested at 73°F and 20°F exhibited brittle failures, and those tested at 110°F exhibited softening type failures.
3. All PC cylinders subjected to compression failed due to a system of cracks along planes inclined at approximately 45° to the vertical axis, indicating failure precipitated by local shear failure.
4. At each of the three test temperatures, the fatigue life of the PC beams increased as the applied maximum stress level decreased. The power model for the S-N relations for PC at three test temperatures provided good correlation with experimental data.
5. The test temperature had significant influence on the fatigue life of the PC. While being subjected to the same maximum stress ratio, the beams tested at 20°F showed the highest fatigue life, and those tested at 73°F had the lowest fatigue life.
6. The mid-span deformation of the PC beams reflected the decrease in stiffness of the beams during the fatigue test. The deformation development for a beam can be divided into three stages. An initial rapid increase in deformation due to crack initiation, a stable deformation development period due to steady-state crack growth, and the final rapid increase in deformations due to unstable crack propagation as the beam approaches its fatigue life.
7. The mid-span deformation at failure for a beam tested at 20°F was only about 10% of that of beams tested at 73°F and 110°F, indicating that the stiffness degradation of PC

material due to fatigue loading is relatively insignificant at 20°F compared to the stiffness degradation at the higher temperatures.

8. Based on the results from the flexural fatigue tests, PC beams tested at 20°F failed in a sudden, brittle manner. All beams tested at 110°F had a softening failure mode. In room temperature tests, the failure mode of some beams tested at lower stress levels changed from brittle failure (in static tests) to softening failure (in fatigue tests). This can be attributed to internal heat build-up resulting from the fatigue loading.

9. Comparison of the initial elastic modulus of PC obtained from the static and flexural fatigue tests showed that at all three temperatures, increasing the loading rate increases the stiffness of the PC, and thus results in an increase in its elastic modulus. The higher the test temperature, the more significant effect the loading rate had on the modulus of PC. At the same temperature, the change in stress level had negligible influence on the observed elastic modulus of PC.

10. The results of the crack repair tests on steel – PC composite specimens indicated that both the Transpo MMA and Pavon asphalt crack sealant can be used to effectively seal the cracks on the PC wearing surface, and thus minimize the potential for infiltration of water onto the deck surface. However, the cracks repaired by both materials reflect on the surface after a very short period of exposure to normal traffic. It was also observed from the tests that the Pavon asphalt sealant had an excellent ability to penetrate small cracks. The MMA material was relatively more viscous, and could not fully infiltrate fine cracks. Observations from the recent field inspections also showed that the Pavon asphalt crack sealant performs marginally better than MMA sealant in infiltrating fine cracks on the wearing surface, and thus provides better protection for the steel deck from the penetration of water.

11. The results from the repair tests also showed that the precracked composite beams bonded by SIMCON fiber reinforced concrete plate performed very well while being subjected simultaneously to fatigue loading and cold temperature cycling. Repair of the PC wearing surface using SIMCON plate bonding technique holds good promise. This type of repair involves substantially more effort than crack sealing with either MMA or Pavon materials and is to be applied to the entire deck surface (not just at crack locations). However, increases in dead load of the wearing surface as well as

an increase in deck stiffness are two issues that need to be considered while choosing this option.

12. Theoretical study performed using orthotropic deck plate theory showed that the maximum bending moment in the deck plate due to traffic load occurred over the longitudinal stiffener. The maximum tensile stress in the top fiber of the wearing surface was computed as 1,085 psi when the PC temperature was between 100°F and 165°F, and 1,846 psi when the temperature was between 0°F and 35°F. These wearing surface stresses agree very well with the in-service PC stresses obtained from the field strain measurement.

13. Thermal stress in PC wearing surface caused by the difference in thermal expansions between the two webs of the south box girder of the eastbound bridge, and by the differences in coefficients of thermal expansion and elastic modulus between steel deck and PC was computed as 1,175 psi. This tensile stress is the most likely cause for the transverse tensile cracks observed in eastbound lanes of the PC wearing surface on the Poplar Street Bridge.

4.2 Recommendations

Of the crack-repair procedures investigated, use of Pavon to seal the cracks in a timely manner appears to be the most practical and cost effective technique, particularly for very fine cracks (such as longitudinal fatigue cracks over stiffeners). For larger transverse cracks, MMA injection into such cracks is perhaps the most effective. In either case, it is expected that the repaired crack will open again after a few hundred cycles of fatigue loading. These materials provide only temporary measures to minimize infiltration of water and deicing salts onto the steel deck plate. Such repairs are best completed under cold (and dry) conditions (early winter) so as to have the cracks open to their maximum widths. While it is not possible to predict "the remaining life" of the wearing surface given the complexity of the problem, the number of variables involved and their associated uncertainties, it is anticipated that with timely and regular repairs using these materials, the PC wearing surface on the Poplar Street Bridge will be serviceable for several more years.

Bonding of precast fiber reinforced concrete (SIMCON – Slurry infiltrated steel fiber mat reinforced concrete) plates as a means of repairing the entire deck appears to hold promise based on the limited number of tests conducted in this study. This repair approach is essentially intended to be a long-term solution to the problem. Further studies are needed to develop an efficient system to apply the plates under field conditions. Unlike repair of cracked epoxy wearing surface, these bonded plates allow use of conventional crack repair techniques normally used for conventional reinforced concrete decks. Additionally, use of precast plates can lend itself well for rapid maintenance operations, should emergencies arise.

LIST OF REFERENCES

[1] American Institute of Steel Construction, "Design Manual for Orthotropic Steel Plate Deck Bridges," AISC, New York, NY, November, 1962.

[2] Gopalaratnam, V. S., Baldwin, J. W., Hartnagel, B.A., and Rigdon, R. L., "Evaluation of Wearing Surface Systems for Orthotropic Steel-plate-bridge Decks," Missouri Cooperative Highway Research Program Report. 89-2, University of Missouri-Columbia, Columbia, Missouri.

[3] Gopalaratnam, V. S., Baldwin, J. W. and Krull, T., "Application of Polymer Concrete Wearing Surface on the Poplar Street Bridge Deck: Construction Report," Missouri Cooperative Highway Research Program Report 92-5, University of Missouri-Columbia, Columbia, Missouri.

[4] Gopalaratnam, V. S., Baldwin, J. W., Hartnagel, B.A., and Krull, T., "Performance of Polymer Concrete Wearing Surface System on the Poplar Street Bridge : Inspection Report I," Missouri Cooperative Highway Research Program Report 92-5., University of Missouri- Columbia, Columbia, Missouri.

[5] Gopalaratnam, V. S., Baldwin, J. W., Hartnagel, B.A., and Holder, M.., "Performance of Polymer Concrete Wearing Surface System on the Poplar Street Bridge : Inspection Report II," Missouri Cooperative Highway Research Program Report 92-5., University of Missouri- Columbia, Columbia, Missouri.

[6] Gopalaratnam, V. S., Baldwin, J. W., Hartnagel, B.A., and El-Shakra, Z.M.., "Performance of Polymer Concrete Wearing Surface System on the Poplar Street Bridge : Inspection Report III," Missouri Cooperative Highway Research Program Report 92-5., University of Missouri- Columbia, Columbia, Missouri.

[7] Gopalaratnam, V. S., Baldwin, J. W., Cao, W.M., Hartnagel, B.A., and El-Shakra, Z.M.., "Performance of Polymer Concrete Wearing Surface System on the Poplar Street Bridge : Inspection Report IV," Missouri Cooperative Highway Research Program Report 92-5., University of Missouri- Columbia, Columbia, Missouri.

[8] Cao, W.M., "Polymer Concrete Wearing Surface System for Orthotropic Steel Plate Bridges," M.S. Thesis, University of Missouri-Columbia, Columbia, Missouri, May 1998.

[9] Rigdon, R. L., "Wearing Surface for Orthotropic Steel Plate Bridges," M. S Thesis, University of Missouri-Columbia, Columbia, Missouri, August, 1990.

[10] Hartnagel, B. A., "Long Term Deck Strain Measurements on an Orthotropic Steel-Plate Bridge Deck," M. S. Thesis, University of Missouri-Columbia, Columbia, Missouri, May. 1993

[11] ACI Committee 503, "Use of Epoxy Compounds with Concrete," ACI Manual of Concrete Practice, 1992.

[12] ASTM D 3633, "Standard Test Method for Electrical Resistivity of Membrane Pavement Systems," American Society for Testing and Materails, ASTM D-3633-88, Vol. 04.03.

[13] ASTM D 4580, "Standard Practice for Measuring Delaminations in Concrete Bridge Decks by Sounding," American Society for Testing and Materials, ASTM D-4580-86, Vol. 04.36.

[14] ASTM C-579, "Standard Test Method for Compressive Strength of Chemical-Resistant Mortars, Grouts, Monolithic Surfacings and Polymer Concretes," American Society for Testing and Materials, ASTM C-579-91, Vol. 04. 05.

[15] ASTM C 580, "Standard Test Method for Flexural Strength and Modulus of Elasticity of Chemical - Resistant Mortars, Grouts, Monolithic Surfacings, and Polymer Concretes," American Society for Testing and Materials, ASTM C 580 - 91, Vol. 04. 05.

[16] James, K.C., "Flexural response of Hybrid High Performance Cement Composite Systems," CE 350 Honors Report, Advisor: Dr. V. S. Gopalaratnam, University of Missouri-Columbia, columbia, Missouri, June 1996.

[17] Timoshenko, S., "Analysis of Bi-metal Thermostats," Journal of Optical Society of America and Review of Scientific Instruments, Vol. 11, No. 6, February, 1926, pp. 233-255.